



The Graduate Institute of Sciences and Engineering

M.Sc. Thesis in Material Science and Mechanical Engineering

**OPTIMIZATION OF CERIUM-IRIDIUM MIXED
OXIDES ARE USED AS CATALYST SUPPORT IN PEM
TYPE FUEL CELLS**

by

Salih VEZİROĞLU

September 2014
Kayseri, Turkey

**OPTIMIZATION OF CERIUM-IRIDIUM MIXED OXIDES ARE
USED AS CATALYST SUPPORT IN PEM TYPE FUEL CELLS**

by

Salih VEZİROĞLU

A thesis submitted to

the Graduate Institute of Sciences and Engineering

of

Melikşah University

in partial fulfillment of the requirements for the degree of

Master of Science

in

Material Science and Mechanical Engineering

September 2014
Kayseri, TURKEY

APPROVAL PAGE

This is to certify that I have read the thesis entitled “**OPTIMIZATION OF CERIUM-IRIDIUM MIXED OXIDES ARE USED AS CATALYST SUPPORT IN PEM TYPE FUEL CELLS**” by Salih VEZİROĞLU and that in my opinion it is fully adequate, in scope and quality, as a thesis for the degree of Master of Science in Material Science and Mechanical Engineering, the Graduate Institute of Science and Engineering, Melikşah University.

September 1, 2014

Asst. Prof. Dr. Furkan DÜNDAR
Supervisor

I certify that this thesis satisfies all the requirements as a thesis for the degree of Master of Science.

September 1, 2014

Prof. Dr. M. Halidun KELEŞTEMUR
Head of Department

Examining Committee Members

Title and Name		Approved
Asst. Prof. Dr. Furkan DÜNDAR	September 1, 2014	_____
Prof. Dr. Mahmut D. MAT	September 1, 2014	_____
Asst. Prof. Dr. Halil ŞAHAN	September 1, 2014	_____

It is approved that this thesis has been written in compliance with the formatting rules laid down by the Graduate Institute of Science and Engineering.

Prof. Dr. M. Halidun KELEŞTEMUR
Director

September, 2014

OPTIMIZATION OF CERIUM-IRIDIUM MIXED OXIDES ARE USED AS CATALYST SUPPORT IN PEM TYPE FUEL CELLS

Salih VEZİROĞLU

M.S. Thesis – Material Science and Mechanical Engineering
September 2014

Supervisor: Asst. Prof. Dr. Furkan DÜNDAR

ABSTRACT

In this study, a durable catalyst support is developed to against the platinum dissolution, the platinum agglomeration and carbon corrosion problems which are commonly seen during long term operations at the catalyst layer of PEM Type Fuel Cell. Cerium-Iridium Mixed Metal Oxides catalyst support was used instead of commonly used Vulcan XC-72 carbon.

Cerium- Iridium Mixed Metal Oxides are prepared at different molar ratios and applied different calcinations. The effect of different support material us on Fuel Cell durability was investigated after the catalyst supports preparation optimization. In this study, analytical methods like XRD, XRF, BET and 4-Probe Conductivity was used for material characterization and Durability Measurement was used for in-situ analysis.

After several analysis and tests the Ir_3CeO_x (75% Iridium- 25% Cerium) synthesized at 400°C and 500 °C and 6 hours shown high performance after durability tests

Keywords: PEM type Fuel Cell, Catalyst Support, Durability, Cerium, Iridium, Metal Oxides

PEM TİPİ YAKIT HÜCRELERİNDE KATALİZÖR DESTEK MALZEMESİ OLARAK KULLANILAN SERYUM-İRİDYUM KARIŞIK METAL OKSİTLERİNİN OPTİMİZASYONU

Salih VEZİROĞLU

Yüksek Lisans Tezi – Malzeme Bilimi ve Makina Mühendisliği
Eylül 2014

Tez Yöneticisi: Yrd. Doç. Dr. Furkan DÜNDAR

ÖZ

Bu tez çalışmasında, PEM tipi yakıt hücrelerinin katalizör tabakasında özellikle uzun süreli çalışma durumunda sıklıkla görülen platin çözünmesi, platin topaklaşması ve karbon korozyonu sorunlarına karşı dayanıklı katalizör destek malzemesi geliştirilmeye çalışılmıştır. Bu amaçla yaygın olarak kullanılan Vulcan XC-72 karbon karası katalizör destek malzemesi yerine Seryum-Iridyum Karışık Metal Oksit katalizör destek malzemesi kullanılmıştır.

Seryum- Iridyum karışık metal oksit katalizör destek malzemeleri farklı oranlarda hazırlanmış ve bunlara farklı süreli ısı işlemler uygulanmıştır. Destek malzemesi hazırlama işlemi optimize edildikten sonra bu destek malzemeleri kullanılarak yakıt hücresinin dayanıklılığına etkisi incelenmiştir. Bu tez çalışmasında, XRD, XRF, BET ve 4-Nokta İletkenlik gibi analitik yöntemlerle malzeme karakterizasyonu ve dayanıklılık ölçümleri gibi in-situ analizler yapılmıştır.

Yapılan analizler ve testler sonucunda 400°C ve 500 °C 'de 6 saat süre ile sentezlenen Ir_3CeO_x (%75 Iridyum -%25 Seryum) katalizör destek malzemeleri dayanıklılık testleri sonucunda yüksek performans göstermiştir.

Anahtar Kelimeler: PEM Yakıt Hücresi, Katalizör Destek, Dayanıklılık, Seryum, Iridyum, Metal Oksitler

DEDICATION

Dedicated to my family for their endless support and patience during the forming phase of this thesis.

ACKNOWLEDGEMENT

I would like to thank Ministry of Science, Industry and Technology that has supported my thesis studies under the project number 01575.STZ.2012-2

My special thanks to my advisor, Asst. Prof. Dr. Furkan DÜNDAR for his encouragement, motivation, guidance, and help on technical issues. Through his help, I get opportunities to learn new things in the development of the thesis.

TABLE OF CONTENT

ABSTRACT.....	iii
ÖZ	iv
DEDICATION.....	v
ACKNOWLEDGEMENT	vi
TABLE OF CONTENT.....	vii
LIST OF FIGURES	x
LIST OF TABLES	xii
LIST OF SYMBOLS	xiii
CHAPTER 1 INTRODUCTION	1
1.1. Energy Sources and Fossil Fuels.....	1
1.2. What is the fuel cells?	1
1.3. History of fuel cells.....	2
1.4. Types of Fuel Cells	2
1.4.1. Alkaline Fuel Cell (AFC).....	5
1.4.2. Phosphoric Acid Fuel Cell (PAFC).....	5
1.4.3. Molten Carbonate Fuel Cell (MCFC)	6
1.4.4. Solid Oxide Fuel Cell (SOFC)	6
1.4.5. Polymer Electrolyte Membrane (PEMFC).....	7
CHAPTER 2 FUEL CELL THERMODYNAMICS	9
2.1. Introduction	9
2.2. Basic Reactions	9
2.3. Thermodynamics of Fuel Cell.....	10
2.4. Theoretical Fuel Cell Efficiency	11
2.5. Voltage Losses	12

2.5.1.	Activation Losses	13
2.5.2.	Ohmic Losses	14
2.5.3.	Mass Transfer Losses	14
2.5.4.	Internal Current and Fuel Crossover Losses	15
2.5.5.	Losses After the Voltage	15
CHAPTER 3 MAIN CELL COMPONENTS		17
3.1.	Membrane Electrode Assembly (MEA).....	18
3.1.1.	Membrane	18
3.1.2.	Catalyst.....	19
3.1.3.	Catalyst Support	20
3.2.	Gas Diffusion Layer (GDL)	20
3.3.	Bipolar Plate.....	21
3.4.	Gasket.....	21
CHAPTER 4 TECHNICAL CHALLENGES IN PEM FUEL CELL.....		22
4.1.	Durability	22
4.1.1.	Catalyst.....	22
4.1.2.	Membranes	26
4.1.3.	Bipolar Plates	26
4.2.	Cost	27
CHAPTER 5 EXPERIMENTAL RESULTS		29
5.1.	Synthesis of Catalyst Support Materials	29
5.1.1.	X-Ray Diffraction (XRD) Analysis	31
5.1.2.	X-Ray Fluorescence (XRF) Analysis.....	36
5.1.3.	Brunauer Emmett Teller (BET) Surface Area Analysis	36
5.1.4.	4–Probe Conductivity Measurements	37
5.2.	Synthesis of Pt/ CeO ₂ -IrO ₂	39
5.3.	Synthesis of Pt-Au/ CeO ₂ -IrO ₂	40
5.4.	Oxygen Reduction Reaction Change of Kinetics Activity	42

CHAPTER 6 CONCLUSION	47
REFERENCES	48

LIST OF FIGURES

FIGURE

Figure 1.1 A schematic diagram of PEM Fuel Cell configuration	7
Figure 2.1 Hydrogen-Oxygen fuel cell performance curve at equilibrium	13
Figure 3.1 Examples of a complete MEA (Fuel Cell Store).....	18
Figure 3.2 Unit molecular structure for a DuPont Nafion electrolyte. [13].....	18
Figure 3.3 Graphical representation of the reaction sites	19
Figure 3.4 Scanning Electron Microscope images of GDL coated Teflon [15].....	20
Figure 4.1 Platinum agglomeration process	24
Figure 4.2 Cost reduction of PEM type of Fuel Cells in time. [46].....	27
Figure 4.3 Breakdown of the 2013 projected fuel cell stack cost at 1,000 and 500,000 systems per year. [46]	28
Figure 5.1 Process of Synthesis of Catalyst Support Materials.....	31
Figure 5.2 XRD pattern of 1-CeO _x synthesized at 400 °C and 6 hours	32
Figure 5.3 XRD pattern of 2-IrCe ₃ O _x synthesized at 400 °C and 6 hours	32
Figure 5.4 XRD pattern of 2-IrCe ₃ O _x synthesized at 500 °C and 6 hours	33
Figure 5.5 XRD pattern of 3-IrCeO _x synthesized at 400 °C and 6 hours.....	33
Figure 5.6 XRD pattern of 3-IrCe ₃ O _x synthesized at 500 °C and 6 hours	34
Figure 5.7 XRD pattern of 4-Ir ₃ CeO _x synthesized at 400 °C and 6 hours	34
Figure 5.8 XRD pattern of 4-Ir ₃ CeO _x synthesized at 500 °C and 6 hours	35
Figure 5.9 XRD pattern of 5-IrO _x synthesized at 400 °C and 6 hours	35
Figure 5.10 XRD pattern of 5-IrO _x synthesized at 500 °C and 6 hours	36
Figure 5.11 Process of Synthesis of Electrocatalyst.....	40
Figure 5.12 Process of Synthesis of Pt-Au Electrocatalyst	41
Figure 5.13 Rotating voltammetry experiment before and after the durability test for M34.....	42

Figure 5.14 Rotating voltammetry experiment before and after the durability test for M35	43
Figure 5.15 Rotating voltammetry experiment before and after the durability test for M44-1.....	43
Figure 5.16 Rotating voltammetry experiment before and after the durability test for M45	44
Figure 5.17 Rotating voltammetry experiment before and after the durability test for M44-2.....	44

LIST OF TABLES

TABLE

Table 1.1 Properties of Fuel Cell Types	4
Table 2.1 Thermodynamics Values in the PEM Fuel Cell [1].....	11
Table 2.2 Potential losses at an example system [12].....	15
Table 3.1 Basic PEM Fuel Cell Components	17
Table 5.1 Molar ratios of synthesized samples	30
Table 5.2 Parameters of Calcination	30
Table 5.3 XRF results of samples	36
Table 5.4 BET results of samples	37
Table 5.5 Four-Probe Conductivity Measurements results of samples	38
Table 5.6 Limit current density of samples	45
Table 5.7 Reduction of limit current after durability test	45
Table 5.8 Reduction of kinetic current performance after durability test.....	46

LIST OF SYMBOLS

SYMBOLS

η_t	Thermodynamic Efficiency
ΔG	Gibbs Free Energy Change
ΔH	Enthalpy Change
T	Temperature
S	Entropy
V	Working Potential
V_{tn}	Thermoneutral Voltage
V_{teo}	Gibbs Free Energy Theoretical Voltage
n	Number of Electron Transferred
F	Faraday Constant
I	Current Density
η_{HHV}	High Heating Value Kinetic Efficiency
η_{LHV}	Low Heating Value Kinetic Efficiency
S_{fuel}	Stoichiometry of Fuel
η_P	Practical Efficiency
η_{PHHV}	Practical High Heating Value Kinetic Efficiency
η_{PLHV}	Practical Low Heating Value Kinetic Efficiency
OCV	Open Circuit Voltage
I_o	Exchange Current Density
R	Ideal Gas Constant
α	Charge Coefficiency

R_i	Internal Resistance
i_l	Limit Current Density
i_{loss}	Loss Current Density

CHAPTER 1

INTRODUCTION

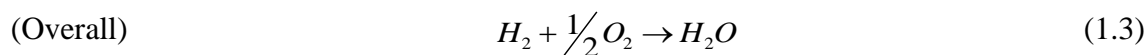
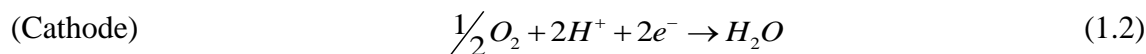
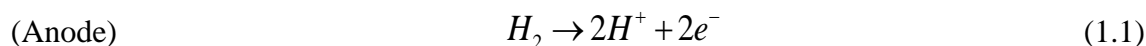
1.1. Energy Sources and Fossil Fuels

People spend energy in many ways to meet the daily needs. People's needs for energy are increasing with each passing day. Today, world meets energy needs from fossil fuels. Fossil fuels are running out quickly and make pollution for environment. As product of the combustion of fossil fuels, SO₂, CO₂ and NO₂ gas's quantity in atmosphere is increasing with each passing day. These gases cause acid rain, to damage the ozone layer, greenhouse effect and to increase the quantity of volatile organic compounds in atmosphere. We need alternative energy sources to reduce environmental damage and avoid irreversible climate issues. An alternative energy conversion technology such as the fuel cell technology offers an attractive possibility for reducing air pollution.

1.2. What is the fuel cells?

A fuel cell is a devices that converts chemical energy of fuel directly into electricity.[1] It has an electrolyte, negative and positive electrodes; called, respectively, the anode and cathode. [1] A fuel cell is in some aspect similar to a battery. However, unlike a battery, fuel cell is just converting system, which a continuous supply of fuel and oxidant. Also the electrodes in a fuel cell do not undergo chemical changes. [1, 2]

In the fuel cell reaction is spread two electrochemical half reaction. [1]



In these reactions, the electrodes transferred from the fuel are forced to flow through an external circuit and do useful work before they can complete the reaction. Because of the direct energy conversion fuel cell works at a higher efficiency than the conventional heating cycle. [2] While fuel cells present high efficiency, they also pass the same serious disadvantages. Cost represents a major problem to fuel cell commercialization. [1]

1.3. History of fuel cells

The history of fuel cells started in 19th century. C.F. Scheonbein was the first to publish results of experiments about the fuel cell concept in 1839. [3] [4] However, the idea of generating electric current from hydrogen and oxygen was first demonstrated by William Grove at the same years. He discovered that by reversing the electrolysis of water recombining hydrogen and oxygen suitable electric current can be produced. [1]

Though the idea of fuel cell had been known for 100 years. It was not used until General Electric developed the first practical fuel cell for U.S. Space Program in the early 1960s. [1] [3] [4] In 1993, Ballard power systems demonstrated fuel cell-powered buses [1] Nowadays the numbers of fuel cell related patents worldwide, but primarily in the United States and Japan, is increasing dramatically. [1]

1.4. Types of Fuel Cells

Fuel cells are classified according to the electrolyte employed. The five most common fuel cell types are; [5]

- Alkaline Fuel Cell (AFC)
- Phosphoric Acid Fuel Cell (PAFC)
- Molten Carbonate Fuel Cell (MCFC)

- Solid – Oxide Fuel Cell (SOFC)
- Polymer Electrolyte Membrane Fuel Cell (PEMFC)

PEMFC and PAFC are fuel cells in which protons move to the cathode, producing water and heat. AFC, MCFC, SOFC are fuel cells in which negative ions travel through the electrolyte to the anode where they combine with hydrogen to generate water and electrons. They can be classified according to used fuel. Direct fuel cells, in which is fed directly to the anode; indirect fuel cells, in which external reforms are used; and finally the regenerative types, in which the fuel cell product is reconverted into reactants and recycled. [6]

While all five fuel cell types are based upon the same underlying electrochemical principles. They all operates at different temperature regimes, in corporate different materials and often differ in their fuel tolerate and performance characteristic, as shown in table 1.1. [7]

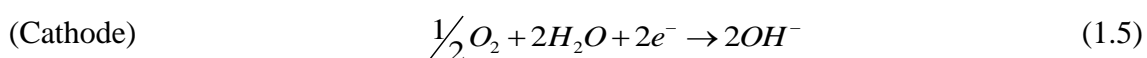
Table 1.1 Properties of Fuel Cell Types

Fuel Cell Type	Electrolyte	Charge Carrier	Operating Temperature	Fuel	Electric Efficiency (System)	Power Range / Application
Alkaline FC (AFC)	KOH	OH ⁻	50-250 °C	Pure H ₂	35-55%	<kW, military, space
Phosphoric Acid FC (PAFC)	Phosphoric Acid	H ⁺	~220 °C	Pure H ₂ (tolerates CO) approx. 1 % CO	40%	CHP (200kW)
Molten Carbonate FC (MCFC)	Lithium and potassium carbonate	CO ₃ ²⁻	~650 °C	H ₂ , CO, CH ₄ , other hydrocarbon (tolerates CO ₂)	>50%	200 kW-MW range, CHP and stand-alone
Solid Oxide FC (SOFC)	Solid oxide electrolyte (yttrian, zirconia)	O ²⁻	~1000 °C	H ₂ , CO, CH ₄ , other hydrocarbon (tolerates CO ₂)	>50%	2 kW-MW range, CHP and stand-alone
Proton Exchange Membrane FC (PEMFC)	Solid Polymer (Such as Nafion)	H ⁺	60-120 °C	Pure H ₂ (tolerates CO ₂)	35-50%	Automotive CHP (5-250 kW), portable

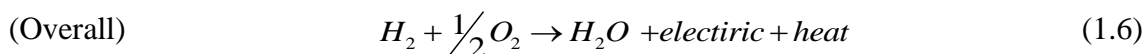
CHP: Combined heat and power

1.4.1. Alkaline Fuel Cell (AFC)

During long years, alkaline fuel cells used by NASA on the space missions. The AFC operates between 50-250°C. The cells use alkaline potassium hydroxide (KOH) as the electrolyte. The concentration of the electrolyte varies from 30-45% to 85%. One of the advantages is that non-precious metals can be used as electrodes and no particular materials are needed.[8] The chemical reactions at the anode and cathode side in an alkaline fuel cell are shown below.



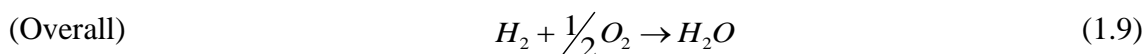
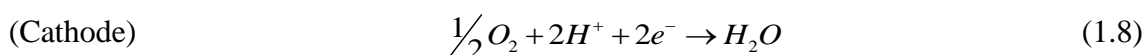
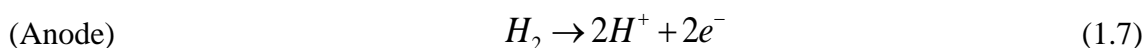
Hydroxyl ions, OH^- , are the conducting species in the electrolyte. The equivalent overall cell reaction is,



Since KOH has the biggest conductance among the alkaline hydroxides, it is the preferred electrolyte.[9] Also AFC's have the highest electrical efficiency (at nearly 70%) in generating electricity. [10] The major disadvantages of this cell is that it very sensitive to CO_2 and CO poisoning, hence it use with reformed fuels and air is limited. [11]

1.4.2. Phosphoric Acid Fuel Cell (PAFC)

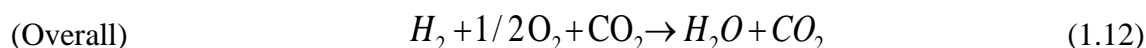
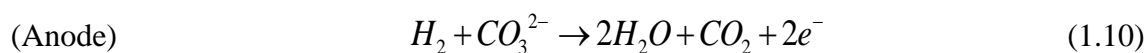
The PAFC operates around 200 °C. Platinum is used in the electrodes and the electrolyte is a colorless viscous phosphoric acid liquid. Efficiency of phosphoric acid fuel cell is about 40%.[11] The chemical reaction at anode and cathode side in a phosphoric acid fuel cell shown below,



The electrochemical reactions occur on highly dispersed electro-catalyst particles supported on carbon black. [9] The PAFC is tolerant to CO₂ and the higher temperature operation is beneficial for co-generation applications.[11] These are the commercially developed types of fuel cells for stationary applications. But development of this types of fuel cell has showed down in the past few years.[9]

1.4.3. Molten Carbonate Fuel Cell (MCFC)

The carbonate fuel cells (MFC) have high operating temperatures almost 650 °C, where carbonates form a highly conductive molten salt with carbonate ions providing ionic conductive molten salt. [1] The chemical reaction at the anode and cathode side in a molten carbonate fuel cell shown below, [9]



The high reaction rates remove need for noble metals catalyst, and gases such as natural gas can be internally reformed without the need for a separate unit. [11] In addition the cell can be made of commonly available sheet metals for less costly fabrication. [11] MCFC generates electricity with up to 50 % efficiency. When washed heat is captured and recycled in the system, the efficiency can be as high as 80 %. [8] These fuel cells are in the pre-commercial stage for stationary power generation. [1]

1.4.4. Solid Oxide Fuel Cell (SOFC)

The SOFC is another highly promising fuel cell that is suitable for high power applications, including industrial and large-scale central electricity generating stations. The SOFC use a solid, nonporous metal oxide, usually Y₂O₃- stabilized ZrO₂ (YSZ) as the electrolyte. [1] The cell operates at 600 – 1000 °C, where ionic conduction by oxygen ions take places. [9] Due to its high temperature operation, high reaction rates are achieved without the need for expensive catalysts, and gases such as natural gas can be internally reformed without the need for fuel reforming. Unfortunately the high operating

temperature limits the materials selection and a difficult fabrication processes results.[11] Similar to MCFC, these fuel cells are in the pre-commercial stage for stationary power generation.[1]

1.4.5. Polymer Electrolyte Membrane (PEMFC)

At the heart of a PEM fuel cell is a polymer membrane that is a thin ($\sim < 50 \mu\text{m}$) proton conductive (such as perfluorosulfanated acid polymer) as the electrolyte.[1] It is impermeable to gases but it conducts protons (hence the name, proton exchange membrane). [1] The function of the proton exchange membrane is to provide a conductive path, while at the same time separating the reactant gases. [9] Membrane is squeezed between the two porous, electrically conductive electrodes, which are generally made of carbon cloth or carbon fiber paper. At the interface between the porous electrode and the proton exchange membrane there is a layer with catalyst particles, generally platinum and platinum alloys supported on carbon. A schematic diagram of PEM Fuel Cell configuration and basic operating principles is shown in Figure 1.1.

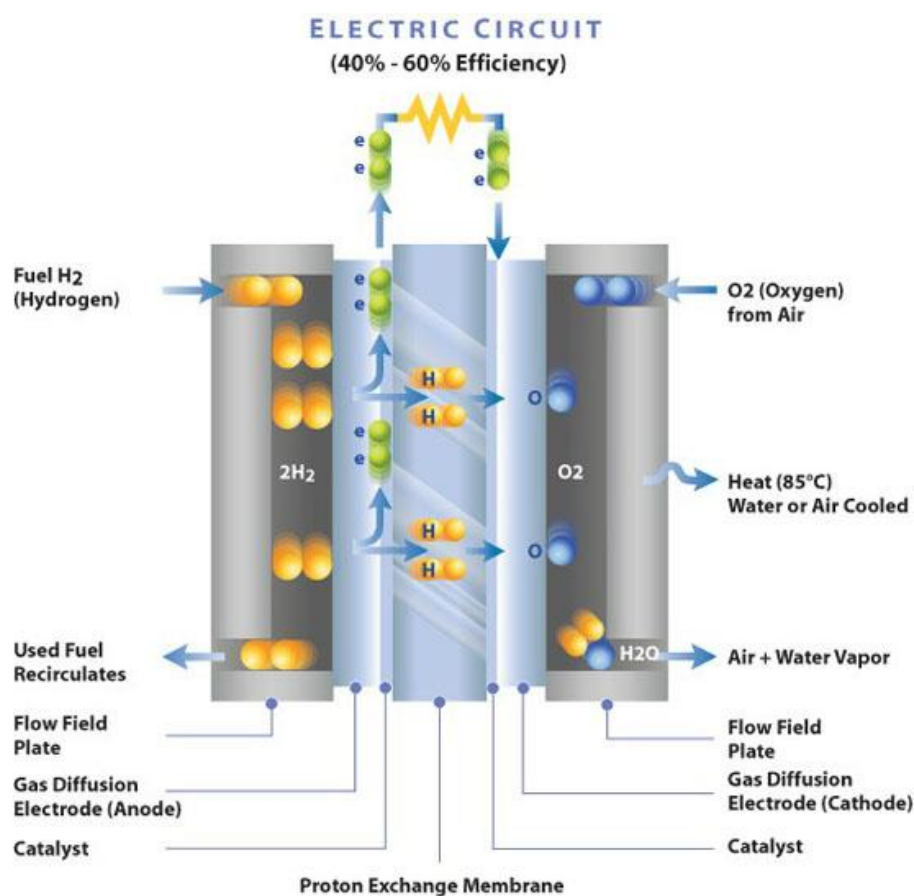


Figure 1.1 A schematic diagram of PEM Fuel Cell configuration

The hydrogen side is negative, called the anode. Oxygen side of the fuel cell is passive, called the cathode. Electrochemical reactions occur at the surface of the catalyst the interface between the electrolyte and membrane. Hydrogen splits into protons and electrons. While the protons move to the cathode through the membrane, the electrons move out of the circuit. At the catalyst sites between the membrane and the other electrode, they meet with the protons and oxygen. Water is created in the electrochemical reaction. This water can be thrown out by hydrogen and oxygen gases. At the end of the reaction direct current is produced.

The PEFC are able to efficiently generate high power densities, thereby making the technology potentially attractive for certain mobile and portable applications.[9] Operating temperature is typically between 60 and 80 °C. [1] However due to the low temperature operation, catalysts (mostly platinum and ruthenium alloys) are needed to increase the rate of reaction.[11] The catalyst is typically platinum supported on carbon.[1] The PEFC is seen as the main fuel cell candidate technology for automotive applications, but also for small- scale distributed stationary power generation, and for portable power applications as well.

CHAPTER 2

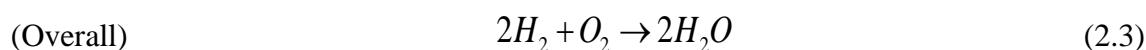
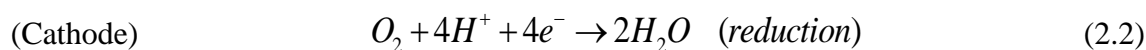
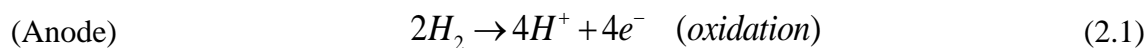
FUEL CELL THERMODYNAMICS

2.1. Introduction

Fuel cells are energy conversion devices. Fuel cells thermodynamics should be known to understanding the conversion of chemical energy into electrical energy.[1, 5] It must obey the laws of thermodynamics

2.2. Basic Reactions

The electrochemical reactions in the fuel cell take place on both sides of membrane. The basic fuel cell reactions are;



On the anode side, hydrogen is oxidized. On the cathode side, oxygen is reduced. These reactions may have several intermediate steps, but these reactions describe the main processes in the fuel cell.

2.3. Thermodynamics of Fuel Cell

Energy difference between reacting a chemical reaction and the products of this reaction express that the change in enthalpy. (ΔH). But practically all of this energy is not released. [1] As result of this reaction, the energy that can be released , is called Gibbs Free Energy (ΔG) and calculated according to equation 2.4 [1]

$$\Delta G = \Delta H - T\Delta S \quad (2.4)$$

T express temperature and S express entropy here. The amount of energy produced by one mole of electron is defined as voltage. A theoretical voltage of the fuel cell can be calculated in accordance with enthalpy, can be calculated in accordance with Gibbs Free Energy too. The voltage value calculated according to changing in enthalpy is called Thermoneutral voltage (V_{tn}), the voltage value calculated according to Gibbs Free Energy theoretical voltage (V_{teo}). Calculation of this expressions are shown in equations 2.5 and 2.6

$$V_{tn} = \frac{-\Delta H}{nF} \quad (2.5)$$

$$V_{teo} = \frac{-\Delta G}{nF} \quad (2.6)$$

Half-reactions taking place both on the anode and cathode side of PEM type Fuel Cells have their each specific enthalpy values as well as Gibbs free energy values. Nevertheless, voltages values formed in anode and cathode are also change. But voltage is not a quantity that may be referred to solely. Voltage should be always expressed in accordance with another voltage value. In literature, the resulting voltage value is always considered to be 0 Volts when a reaction has taken place on the Anode side of a PEM fuel cell. Voltage values that occur in other reaction are always expressed by comparing with this reaction. The enthalpy difference created between the cathode and anode side of a PEM fuel cell, Gibbs Free energy values and the numerical values of Voltage are shown in table 2.1

Table 2.1 Thermodynamics Values in the PEM Fuel Cell [1]

	Temperature (°C)	Change of Enthalpy (ΔH) (kJ/mol)	Gibbs Free Energy (ΔG) (kJ/mol)	Theoretical (V)
High Heating Value	25	-286,02	-237,34	1,23
	60	-284,85	-231,63	1,20
	80	-284,18	-228,42	1,18
Low Heating Value	25	-241,98	-228,74	1,19
	60	-242,37	-226,79	1,18
	80	-242,60	-225,63	1,17

2.4. Theoretical Fuel Cell Efficiency

The efficiency of any conversion devices are defined as the ratio between energy input and useful energy output. [1] Efficiency of an ideal Fuel Cell based upon heat content ΔH is obtained by dividing maximum work out by the enthalpy input, η_t

$$\eta_t = \frac{\Delta G}{\Delta H} \quad (2.7)$$

The maximum thermodynamic efficiency under standard conditions is 83%. ($\Delta G = -237,2$ kJ/mol, $\Delta H = -285,8$ kJ/mol) [4] However, this efficiency value, actually is the theoretical maximum efficiency value and it doesn't seem possible to achieve this value in reality, indeed.

There are main losses occurred during fuel cell reactions, such as activation losses, ohmic losses, mass transfer losses and internal current losses. These losses are obviously the reason of a voltage drop which in theory needs to be happening already. In other words, called Kinetic Efficiency, which is the ratio of the amount of voltage composed on the fuel cell, to the amount of voltage expected to be composed theoretically. This kinetic energy can be calculated in two ways. The product resulted by the reactions taken place in fuel cell may have low energy (liquid water), and giving importance on this issue in calculations gives us the one of the methods called: "high heating value kinetic efficiency (η_{HHV})". Simply and vice versa, resulted products' energy by the reactions taken place in fuel cell may have high energy and giving importance on this issue in

calculations gives us the other method so called: “low heating value kinetic efficiency (η_{LHV})”.

$$\eta_{HHV} = \frac{V}{\frac{-\Delta H_{HHV}}{nF}} \quad (2.8)$$

$$\eta_{LHV} = \frac{V}{\frac{-\Delta H_{LHV}}{nF}} \quad (2.9)$$

On the other hand, to be able to get the more accurate efficiency value, one needs to deal and take the stoichiometry values (S_{Fuel}) of the fuels used in the fuel cell into account. This would be called as Practical Efficiency (η_p). Practical efficiency is also calculated by using high heating value (η_{PHHV}) and low heating value (η_{PLHV}) techniques.

$$\eta_{PHHV} = \frac{1}{S_{Fuel}} \frac{V}{\frac{-\Delta H_{HHV}}{nF}} \quad (2.10)$$

$$\eta_{PLHV} = \frac{1}{S_{Fuel}} \frac{V}{\frac{-\Delta H_{LHV}}{nF}} \quad (2.11)$$

2.5. Voltage Losses

When gases fed to the system and run the cell with a load, without closing the external circuit, the cell potential is expected to be at theoretical value (1,23 V). However, it is lower than theoretical potential due to the losses in the fuel cell and this voltage response is known as open circuit voltage (OCV) [12]

In addition the this loss, there are different kinds of voltage losses in a fuel cell caused by the following factors; [1]

- Activation Losses
- Ohmic (Resistive) Losses
- Mass Transfer Losses

➤ Internal Currents and Fuel Crossover Losses

When current is flowing in PEM fuel cells is increasing potential losses. The current drawn from fuel cell and the potential relation is shown below in Figure 2.1. [4]

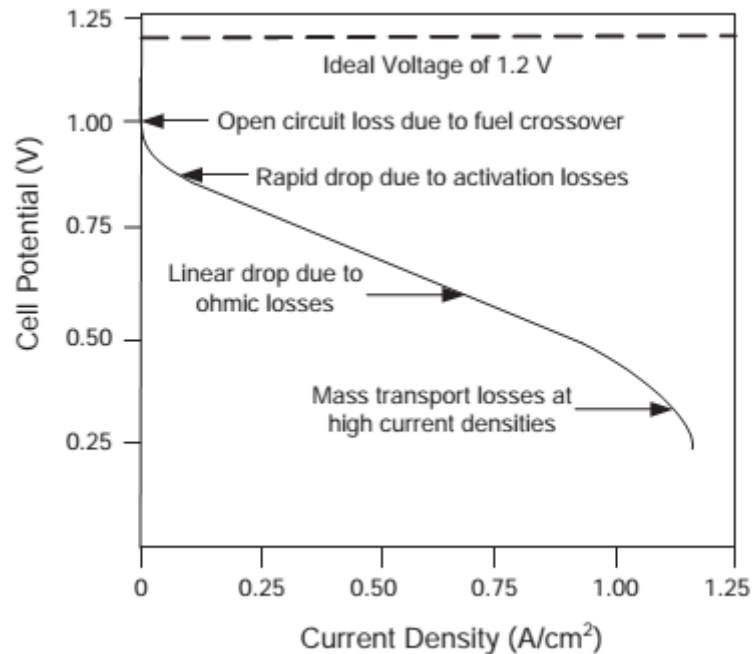


Figure 2.1 Hydrogen-Oxygen fuel cell performance curve at equilibrium

The real voltage output for a fuel cell can be written by this equation,

$$V = E_{theo} - \eta_{act} - \eta_{ohm} - \eta_{conc} \quad (2.12)$$

2.5.1. Activation Losses

Activation losses are those associated with the initial dramatic voltage losses in low temperature fuel cells. Electrochemical reactions in the fuel cell occur the surfaces and involve of electrons. Therefore, the rate of the reaction is proportional to the reaction surface area of catalyst. Some of the catalysts allow that reactions to take place but some cannot because they do not have enough needed activation energy that specific reaction to be taking place. Furthermore, the total activation loss would be calculated by using the equation given below.

$$V = \frac{R \cdot T}{\alpha \cdot F} \ln \left(\frac{i}{i_0} \right) \quad (2.13)$$

In here, i_0 - exchange current density, R - ideal gas constant, T – temperature, α – charge coefficient, n_e – number of electrons transferred, F – Faraday constant and i – current. “Exchange current density” is called the ongoing current density in both directions where no current is drawn. As high as this exchange current density value, the activation loss would be low.

2.5.2. Ohmic Losses

Ohmic losses comes from the flow of ions in the electrolyte and the flow of electrons through the electrically conductive fuel cell components. [12] These losses can be calculated by Ohmic Law's,

$$V = i \cdot R_i \quad (2.14)$$

In here, i – current density ($A \text{ cm}^{-2}$), and R_i –total cell internal resistance ($\Omega \text{ cm}^{-2}$). [1] In order to reduce the value of the ohmic losses it is necessary to use extremely high conductive electrodes.

2.5.3. Mass Transfer Losses

Mass transfer losses occurs when a reactant is rapidly consumed at the high current density. [1] For the higher current density, mass transfer limitations due to the transport limit of reactant gases through the pores of gas diffusion layers, electrocatalyst and accordingly cell voltage drops dramatically. [12] A relationship for voltage loss due to concentration polarization is obtained; [1]

$$V_{ml} = \frac{R \cdot T}{n \cdot F} \ln \left(\frac{i_l}{i_l - i} \right) \quad (2.15)$$

In here, R – ideal gas constant, T – temperature, n – number of electrons transferred, F – faraday constant, i_l - limit current density, i – current density. Mass transfer losses can be minimized by the careful design of a fuel cell's flow channel in bipolar plate.

2.5.4. Internal Current and Fuel Crossover Losses

Although it is generally assumed that the electrolyte is not electrically conductive and impermeable to gases, some small amount of hydrogen and electrons diffuse through the membrane. [4] It can be calculated by this equation 2.16; [1]

$$V = \frac{R \cdot T}{\alpha \cdot F} \ln \left(\frac{i_{loss}}{i_o} \right) \quad (2.16)$$

In here, R – ideal gas constant, T – temperature, n – number of electrons transferred, F – faraday constant, i_{loss} - loss current, i_o – internal current density. These losses may appear in significant in the fuel cell operation. Because, amount of diffused hydrogen is very lower than amount of used hydrogen.

2.5.5. Losses After the Voltage

After considering all voltage losses in the fuel cell, the equation 2.17 can be used to calculate the voltage that occurs in the fuel cell. [1]

$$V_{cell} = V_{theo} - \frac{R \cdot T}{\alpha \cdot F} \cdot \ln \left(\frac{i + i_{loss}}{i_o} \right) - \frac{R \cdot T}{n \cdot F} \cdot \ln \left(\frac{i_L}{i_L - i} \right) - i \cdot R_i \quad (2.17)$$

Table 2.2 Potential losses at an example system [12]

Type of Voltage	Voltage (V)
Thermoneutral Voltage	1,482
Theoretical Open Circuit Voltage	1,208
Practical Open Circuit Voltage	0,998
Activation Losses	-0,391
Ohmic Losses	-0,128
Mass Transfer Losses	-0,022
Internal Current and Fuel Crossover	-0,000
Cell Voltage	0,667

The reason that practical open circuit voltage is lower than the theoretical voltage is that the internal current and fuel crossover amount drops the voltage when no current was drawn from the system. Fuel is used when current starts to retreat from the system so that the effect of this loss is frequently deficient.

CHAPTER 3

MAIN CELL COMPONENTS

A PEM fuel cell is built in a very similar way to other fuel cells. There are two electrodes (cathode and anode), which are on opposite sides of on membrane and bipolar plate. However, there are some significant differences in the materials used in a need for materials with specific properties. Those are demonstrated by table 3.1. [4]

Table 3.1 Basic PEM Fuel Cell Components

Component	Description	Common types
Proton exchange membrane	Enables protons to travel from the anode to the cathode	Persulfonic acid membrane (Nafion 112, 115, 117)
Catalyst layers	Breaks the fuel into protons and electrons	Platinum / carbon catalyst
Gas diffusion layers	Allow the fuel / oxidant to travel through the porous layer	Carbon cloth or Toray paper
Flow field plates	Distributes the fuel / oxidant to the gas diffusion layer	Graphite, stainless steel
Gaskets	Prevent fuel leakage	Silicon, Teflon
End Plates	Holds stack layers in place	Stainless Steel, graphite, polyethylene, PVC

3.1. Membrane Electrode Assembly (MEA)

The MEA consists of polymer membrane electrolyte and two electrodes (anode and cathode) that sandwich the polymer membrane. These components of MEA are compressed by high temperature and pressure. The MEA are very thin and connected in series, usually using bipolar plates.

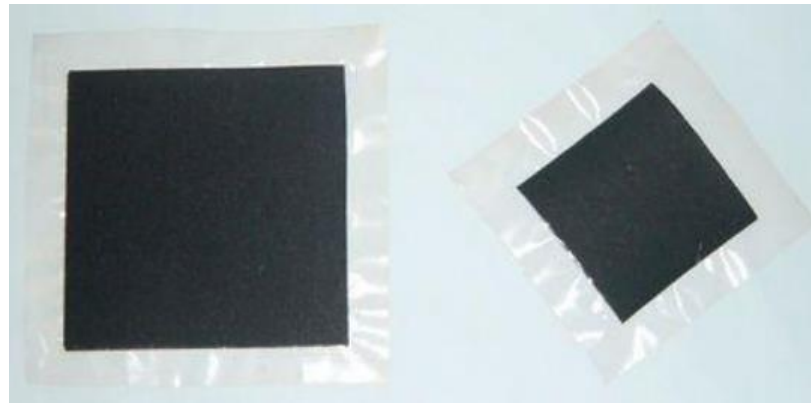


Figure 3.1 Examples of a complete MEA (Fuel Cell Store)

3.1.1. Membrane

An ideal membrane for PEM fuel cell should exhibit excellent proton conductivity, mechanical strength, chemical and thermal stability, low gas permeability, low water drag, low manufacturing cost and good availability. [13] Typically, the membranes for PEM fuel cells are made of perfluorocarbon-sulfonic acid ionomer (PSA). This is essentially a copolymer of tetrafluorethylene (TFE) and various perfluorosulfonate monomers. Commercially membrane material is Nafion by developed DuPont. [1]

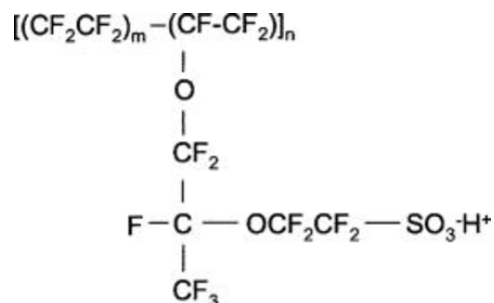


Figure 3.2 Unit molecular structure for a DuPont Nafion electrolyte. [13]

SO_3^- ions with H^+ ions are bonded the end of the side chain. The thickness of the Nafion can be optimized. Although the thinner layer increases proton conductivity and accordingly the performance.[1] However, mechanical strength of membrane becomes weak and cause degradation problems. So the lifetime of the membrane is very critical to determine the life time of the cell. [12]

3.1.2. Catalyst

Electrochemical reaction take place on catalyst surface where there species have access, called “three phase boundary”. It is showed graphically in Figure 3.3. [1]

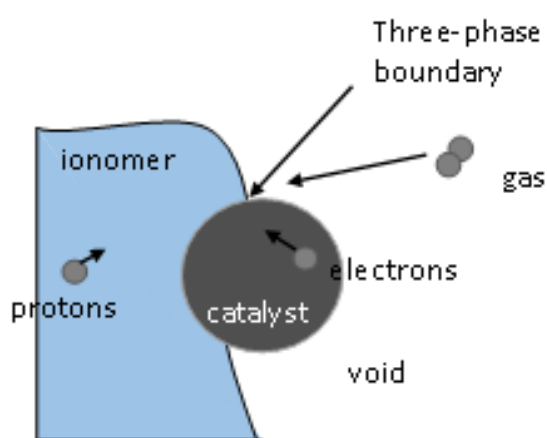


Figure 3.3 Graphical representation of the reaction sites

Electrons travel through electrically conductive solid and protons through ionomer, therefore the catalyst must be intimate contact with the ionomer. In the reaction site voids are present, too and the reactant gases travel through these voids. More precisely the electrodes are porous to allow gases to travel reaction sides. [1]

Platinum is the most common catalyst in PEM fuel cell for both hydrogen oxidation and oxygen reduction. In the early development of fuel cell, the platinum catalyst loading was as high as 28 mg/cm^2 . In recent years, the platinum loading is reduced to less than 1 mg/cm^2 without sacrificing the fuel cell performance or power output. [8] Also, The cost from the catalyst have been decreased by lowering the platinum content significantly, currently around $0,1 \text{ mg/cm}^2$ in anode side $0,5 \text{ mg/cm}^2$ in cathode side. Nowadays, Platinum alloys are being used to reduce platinum loading on the catalyst layer. [14] [15]

3.1.3. Catalyst Support

As small particles (4 nm or smaller) the catalyst's dispersion in the high surface area is very important. For that it is needed high surface area for keeping catalyst and catalyst support having a good conductivity. [1] A widely used carbon-based powder is Vulcan XC72 © (by Cobat). Through this material, the platinum is highly divided and spread out, so that a very high proportion of the surface are can be in contact with the reactant. In this way, the catalyst loading can be reduced greatly.[12]

3.2. Gas Diffusion Layer (GDL)

Gas diffusion layers must be sufficiently porous to allow flow of both reactant gases and water. In addition to, it must be both electrically and thermally conductive. [1] The typical GDL's thickness is in the range of 100 – 300 μm .

The porous gas diffusion layer in PEM fuel cell responsible for, [1]

- Providing a pathway for reactant and product gases from the catalyst layer
- Allowing the electrodes to complete the electron circuit
- Providing the mechanical support to the MEA

Also, in high humidity condition, the GDL assists in the water management by controlling the amount of water to reach and be held at the membrane for hydration. Teflon coating is used in GDL for wet-proof. [16]

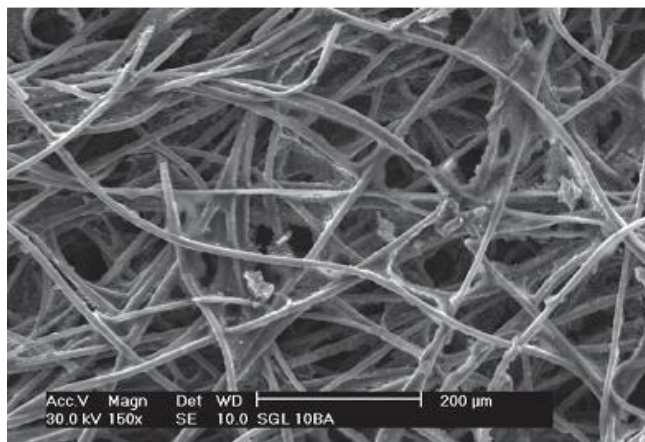


Figure 3.4 Scanning Electron Microscope images of GDL coated Teflon [15]

3.3. Bipolar Plate

Bipolar plates have multiple functions and they are also most costly and problematic component of a PEM fuel cell. These plates on each sides of the MEA are called “end plates” or “flow field plates”. Its primary target is to supply and distribute reactant gases to GDL’s surface through flow channels. Also, bipolar plates should provide electrical connection between the individual cell and GDL.[1]

Bipolar plates should have some specific properties. These are, [1]

- High electrical conductivity – for electron transfer between cells
- Low gas permeability – to prevent loss fuel voltage in case two different gases cross over each other side
- Mechanical strength – to provide structural strength to create cell directory
- Lightness – for use in portable application
- High thermal conductivity – to remove the heat generated in the fuel cell
- Corrosion Resistivity – to become resistant to the acidic environment in fuel cell

The main materials having these features stand out. Many research are carried out about graphite polymer plates that provide all of these features [17] [18] and metallic plates [19].

3.4. Gasket

Gaskets should have some properties in PEM fuel cell. [20] Those are,

- Preventing gas leaking outside from the desired region
- Withstanding acidic environment
- Unreacting with hydrogen and oxygen
- Resisting to melt and breakage
- Not containing substances that poison the catalyst

A sealing material must be used. Silicone, Teflon and Viton seals provide greatly these features.

CHAPTER 4

TECHNICAL CHALLENGES IN PEM FUEL CELL

Fuel cells have the potential to replace the internal-combustion engine in vehicles and provide power in stationary and portable power applications because they are energy-efficient, clean, and fuel-flexible. [9] However, the main hurdles facing the PEM fuel cell industry from commercialization and competing with other power generation system are durability, high cost, optimization of the fuel cell component materials and operating conditions and the fuel availability.

4.1. Durability

Durability is one of the most important issue for commercialization of PEM fuel cell. PEM fuel cells consist of number of different components, such as catalysts, catalyst supports, membranes, gas diffusion layers, bipolar plates and gaskets. To achieve the durability targets for PEM fuel cell systems, it is essential that each of the components has required durability. [21]

4.1.1. Catalyst

In the PEM fuel cell, problems seen in the catalyst layer can be summarized under four main headings.

- Platinum dissolution or oxidation
- Platinum agglomeration

- Carbon corrosion of catalyst support
- Poisoning carbon layer with gases

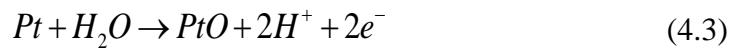
4.1.1.1. Platinum Dissolution

Platinum is the most common catalyst in PEM fuel cell. Platinum may be oxidized in time by the effects work-conditions and may be dissolved and removed from the catalyst layer [22-25]. The first study almost has been made by Pourbaix and he also identified the dissolved amount of Platinum atoms by considering the pH and voltage concepts. [22] By considering the Potential vs. pH diagram (also known as Pourbaix diagrams) for Pt atoms to be dissolved at 25 °C, pH needs to be under 0 and potential needs to be between 1,0-1,2 V. There are two main possibilities which explains the dissolving mechanism of Pt atoms. The first possibility is the ionization of Platinum metal directly. (Equation 4.1). This after-reaction voltage values varies by the Platinum-Ion concentration. That voltage can be calculated by equation 4.2 [26]

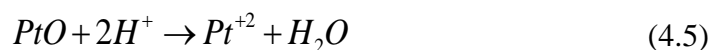


$$E_0 = 1,19 + 0,029 \cdot \log[Pt^{+2}] \quad (4.2)$$

The second possibility is the gradual dissolution of platinum. In the first stage the surface of the platinum atoms are oxidized. (Equation 4.3) After this reaction voltage value is shown depending on pH in equation 4.4. Afterwards, these H⁺ ions attacks to the oxidized surface and results that Platinum atoms ionize and finally they are removed from the surface. (Equation 4.5) The amount of platinum ions that occurs after this reaction changes depending on the pH. (Equation 4.6)



$$E_0 = 0,98 + 0,59 \cdot pH \quad (4.4)$$



$$\log[Pt^{+2}] = -7,06 - 2 \cdot pH \quad (4.6)$$

In the usual working-conditions of PEM type of fuel cells, Platinum catalysts shows a definite behavior in thermodynamic means. Both at the start-up and at the turn-off of the fuel cell, some unexpected issues may occur such as that Platinum particles are being dissolved. [26]

4.1.1.2. Platinum Agglomeration

The reduction of the catalyst layer's active surface area is considered as one of the main reason to drop the performance of PEM fuel cells. It seems that the particle size (increasing the size) don't have a significant effect on lowering the performance. However, the most important effect for the reduction of catalyst active surface area is the catalyst agglomeration. (Figure 4.1)). The agglomeration in the Catalyst part of the PEM fuel cells occurs in two ways. First way being that the Platinum particles move on the Carbon Support Plate and the second being that the catalyst particle's dissolution and removal respectively, finally reaching onto another Platinum particle. [26]

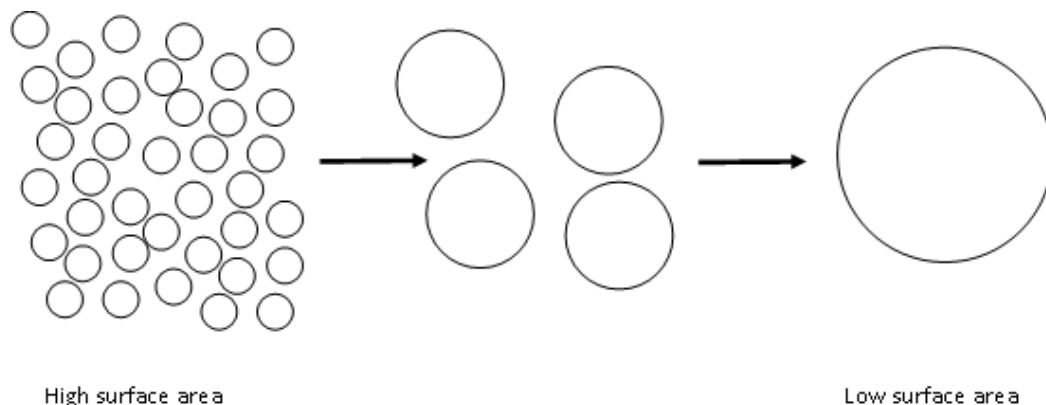


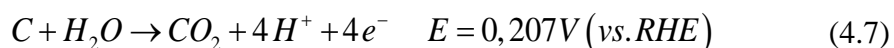
Figure 4.1 Platinum agglomeration process

The voltage values in PEM Fuel Cells are ranging usually in between 0,4 and 1,0 Volts. However, in some circumstances, the potential may go over than 1 Volts. The potential value higher than 0.85 Volts gives the possibility to the Platinum ions to dissolve. The dissolved Platinum particles usually prefers to land on another high-energized Platinum particles. [26] The resulting electrons by the reaction occurred move to the area where the agglomeration happening on the Carbon Support. [26] This agglomeration mechanism is also called so, *Electrochemical Ostwald Ripening type of*

Agglomeration. This type of agglomeration is not seen in Alumina and Silica based catalyst supports.

4.1.1.3. Carbon Corrosion

Carbon is an attractive choice for PEM fuel cell catalyst support material due to its high surface area, high electron conductivity [27]. However, Carbon is readily oxidized to carbon dioxide (CO₂) under certain operation condition. Carbon corrosion occurs via the following reaction. [28]



This reaction is always thermodynamically favorable at the PEM fuel cell. The carbon corrosion process leads to electrically isolated Pt particles that are separated from the support material and also contributes to platinum agglomeration and drop in platinum utilization too. [29]

Therefore, alternative materials instead of carbon-based catalyst support is needed. So, various alternative non-carbon catalyst support have been investigated. Tin oxide (SnO₂) showed high activity for the oxygen reduction reaction [30]. Titanium Oxide (TiO₂) has been shown to exhibit high electrochemical performance and good stability. [31] [32] Indium Tin Oxide (ITO) has been shown to possess high electron conductivity and stability but has lower activity than Pt/C, likely due to its lower surface area leading to poor platinum dispersion. [33] There are other metal oxides that have been used as non-carbon catalyst support. Tungsten Oxide (WO₃) [34] [35] [36], Zirconium Oxide (ZrO₂) [37], Titanium Oxide (Ti₄O₇) [38], Ruthenium – Titanium mixed oxides (RuO_x- TiO_x) [39] [40], Titanium – Tungsten mixed oxides (TiO_x- WO_x) [41], Ruthenium – Silicon mixed oxide (RuO₂- SiO₂). [29] [42]

4.1.1.4. Poisoning of Carbon Layer by Gases

In the PEM type of fuel cells, the hydrogen used in the anode side and the oxygen (or air) used in the Cathode side is not purely (100%) produced. Some impurities inside these gases affects the fuel cell performance and durability, negatively. [43] The hydrogen gas used on the anode side is gained by the electrolysis of water and after some chemical reaction of hydro-carbon. The oxygen used on the Cathode part of the PEM Fuel Cell is

simply taken by the Air. These unwanted substances (impurities) mostly damages the catalyst layer.

These impurities (CO, NH₃, NO₂, SO₂ etc.) are absorbed on Platinum surface, which reduces the active surface area of the catalysts. This dramatically reduces the performance, indeed. Most importantly, the GDL loses its unique surface properties, especially the hydrophobicity quality, by the exposal of this impurities. Expectedly, this causes the water management and the mass transfer issues.

4.1.2. Membranes

In PEM fuel cell membranes with a significant component of the fuel cell are degraded over time. Therefore membrane determines the operating life of the fuel cell. Membranes are subject to two types of degradation. These are physical and chemical degradation. Physical degradation occurs the low creep resistance of the membrane with respect time after, under constant force, as a result of temperature and humidity changes. After physical degradation, micro-cracks and the gas permeability of membrane are increased. The chemical degradation is basically the coating of the membrane's sulfonic acid chains with radicals and ions, in time. After chemical degradation membrane loses acidic functionality and thus its ionic conductivity. [44]

Recent research activities in PEM fuel cell have focused on developing PEM fuel cell operating above 100°C. For this membrane research resisting high temperatures have accelerated.

4.1.3. Bipolar Plates

In PEM fuel cell there are main features that are expected from bipolar platinum. Among these agents hydrogen and oxygen are required to feed not mixing in fuel cell. The purpose of these plates is mainly to supply gas through flow channels to anode and cathode. At the same time, they manage the electron transfer over the gas diffusion layer which are already in contact with these flow channels. Bipolar plates must deal with corrosion issues under the conditions of acidic environment as well as the effect under potential having the range of 0 V and 1,0 V. This causes some significant durability problems. This causes serious stability problems. For this corrosion - resistant graphite bipolar plate is attempted to increase the durability. [45]

Cost must be reduced to the commercialization of PEM fuel cell. By this reason, it is highly desired to replace this final-price very high products (processed graphite plates) with other cost-effective solutions, quick and easy manufactural metal plates. [46]

4.2. Cost

Fuel Cells use catalysts in order to increase the reaction inside the stack. There are many catalysts used in fuel cells but mostly platinum is used because of its stable operation. But nowadays platinum is very expensive and usage of this material increases cost. Especially for automotive applications this is a real problem. Automotive applications use PEM fuel cells so platinum usage in these cells increases production costs of fuel cell powered vehicles. Instead of platinum using an alternative material will decrease the cost. The cost of fuel cell power systems must be reduced before they can be competitive with internal combustion engines.

The target that the United States Department of Energy showed up as a necessary to capture until 2020 is 55 \$/KW. [47] In terms of years PEM fuel cell's cost reduction and targets are shown in figure .This analysis is made to determine a possible cost strategy of a PEM Fuel Cell by considering 80 kW and 500,000 systems. [47]

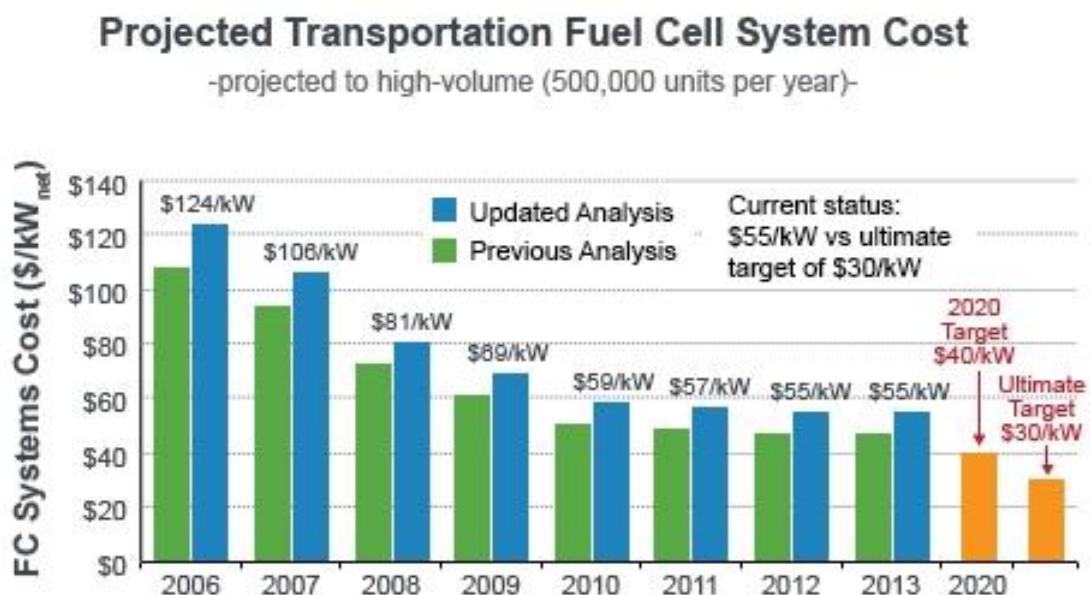


Figure 4.2 Cost reduction of PEM type of Fuel Cells in time. [46]

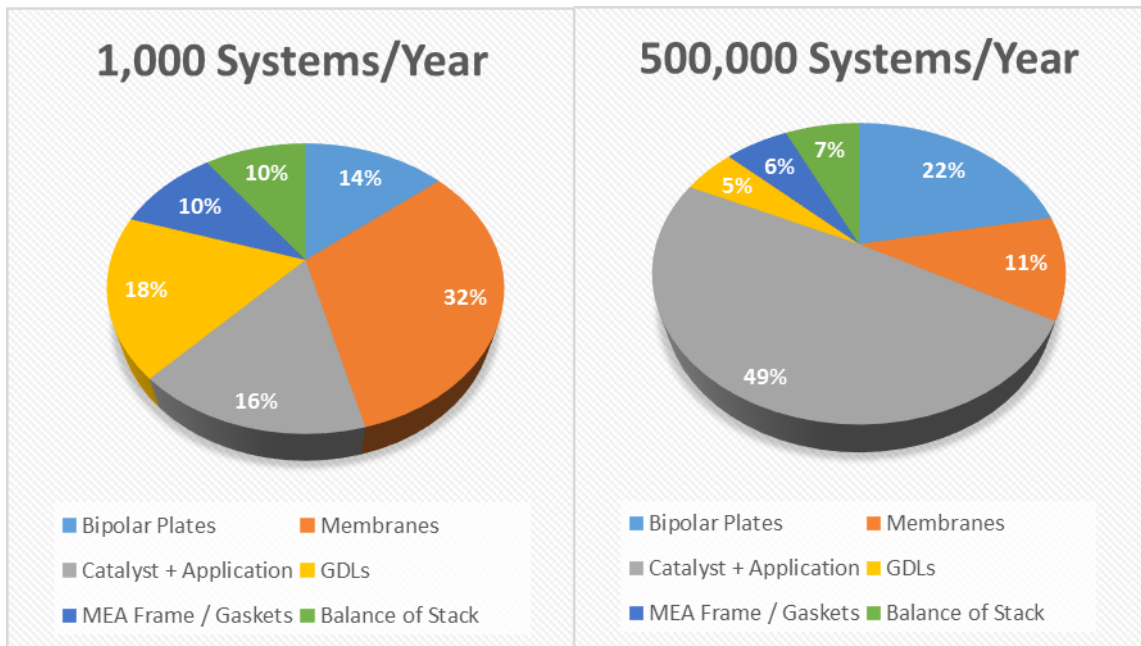


Figure 4.3 Breakdown of the 2013 projected fuel cell stack cost at 1,000 and 500,000 systems per year. [46]

CHAPTER 5

EXPRIMENTAL RESULTS

In this thesis study, the catalyst support materials being Cerium Oxide, Iridium Oxides and Cerium- Iridium Mixed Oxides are optimized and synthesized to be used in PEM fuel cells. During this optimization, X-ray Powder Diffraction (XRD) Analysis, X-Ray Fluorescence (XRF) Analysis and Brunauer Emmett Teller (BET) Surface Area Analyses are used.

5.1. Synthesis of Catalyst Support Materials

The catalyst support materials used in PEM type of fuel cells are expected to have such qualities, having high surface area ($100 \text{ m}^2/\text{g}$) and adequate conductivity are indispensable. In this study, the Sodium Nitrate Fusion method of Adams and his colleagues has been used to achieve the desired catalyst support material synthesis. [48]

To initiate, some percentage values are chosen for Cerium Oxide, Iridium Oxide and Cerium-Iridium Mixed Oxide type of catalyst support materials, as shown table 5.1

Table 5.1 Molar ratios of synthesized samples

	Catalyst Support Material	The molar ratio of Cerium	The molar ratio of Iridium
1	CeO ₂	% 100	% 0
2	IrCe ₃ O _x	% 75	% 25
3	IrCeO _x	% 50	% 50
4	Ir ₃ CeO _x	% 25	% 75
5	IrO ₂	% 0	% 100

Depending on the molar percentage of the catalyst support material, following are taken as needed: Cerium (III) Chloride Heptahydrate, (Alfa Aesar, 99%) and Iridium (III) Chloride Hydrate (Alfa Aesar, 99,9%). These substances are to be mixed up to 20 times of the total mass with 80 times meshed Sodium Nitrate (NaNO₃) and with agate mortar. Afterwards, some amount of water added and will be kept mixing as well. This mixing is added into the ceramic crucible, closing its top with ceramic cover is necessary and then it needs to be furnaced at high temperature for the calcination

Table 5.2 Parameters of Calcination

		Calcination Temperature			
		400 °C	500 °C	600 °C	650 °C
Time	6 hours	✓	✓	✓	
	8 hours	✓	✓	✓	
	10 hours	✓	✓	✓	✓

The component prepared after the heat treatment is taken from the ceramic crucible with the pure water. The aqueous solution needs to be filtered and washed with enough amount of distilled water. Support material left over the filter should be dried in the vacuumed oven overnight at 100 °C. All process can be seen at figure 5.1

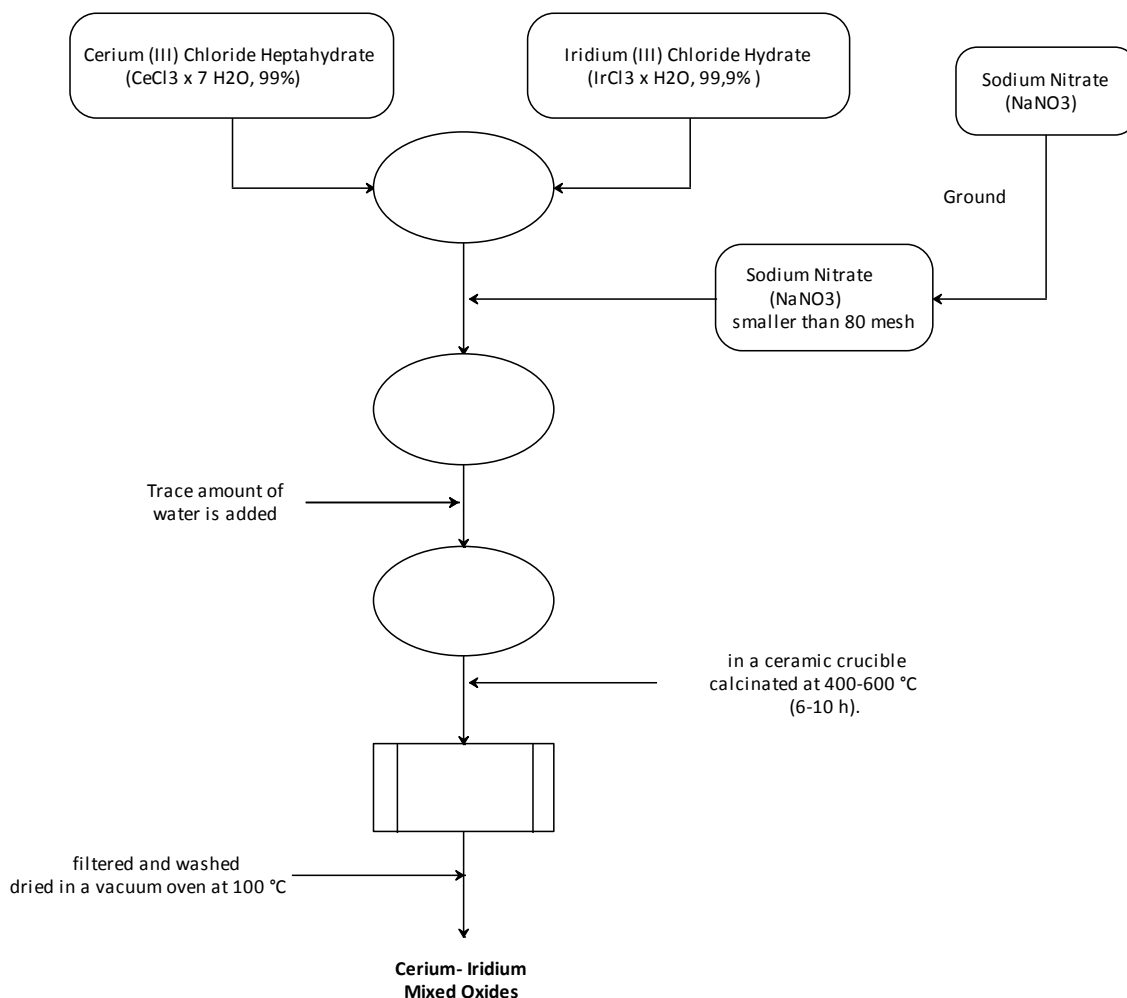


Figure 5.1 Process of Synthesis of Catalyst Support Materials

5.1.1. X-Ray Diffraction (XRD) Analysis

After the XRD results, the CeO_2 (Cerionite) and IrO_2 (Iridium Oxide) are shown as more than usual. However, the characteristic phase angles of the both materials are substantially similar. Iridium oxide phase angle cannot be seen clearly when synthesized especially at $400\text{ }^\circ\text{C}$ and $500\text{ }^\circ\text{C}$ %25 in the Number 2 named catalyst support material. On the other hand, almost 50% Iridium Oxide including Number 3 catalyst support material and, almost 75% Iridium Oxide including Number 4 catalyst support material there is shown a quite amount of Iridium oxide phase obviously. The characteristic peak at $34,5^\circ$ is usually seen in catalyst support materials which are synthesized around $400\text{ }^\circ\text{C}$ and $500\text{ }^\circ\text{C}$. Results are given below.

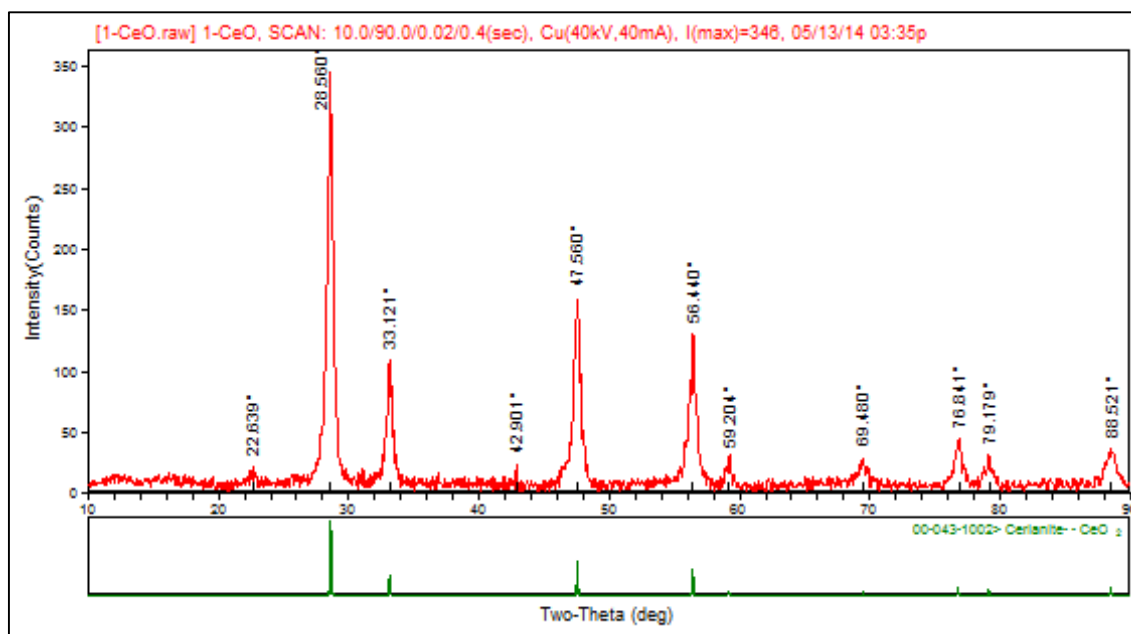


Figure 5.2 XRD pattern of 1-CeO_x synthesized at 400 °C and 6 hours

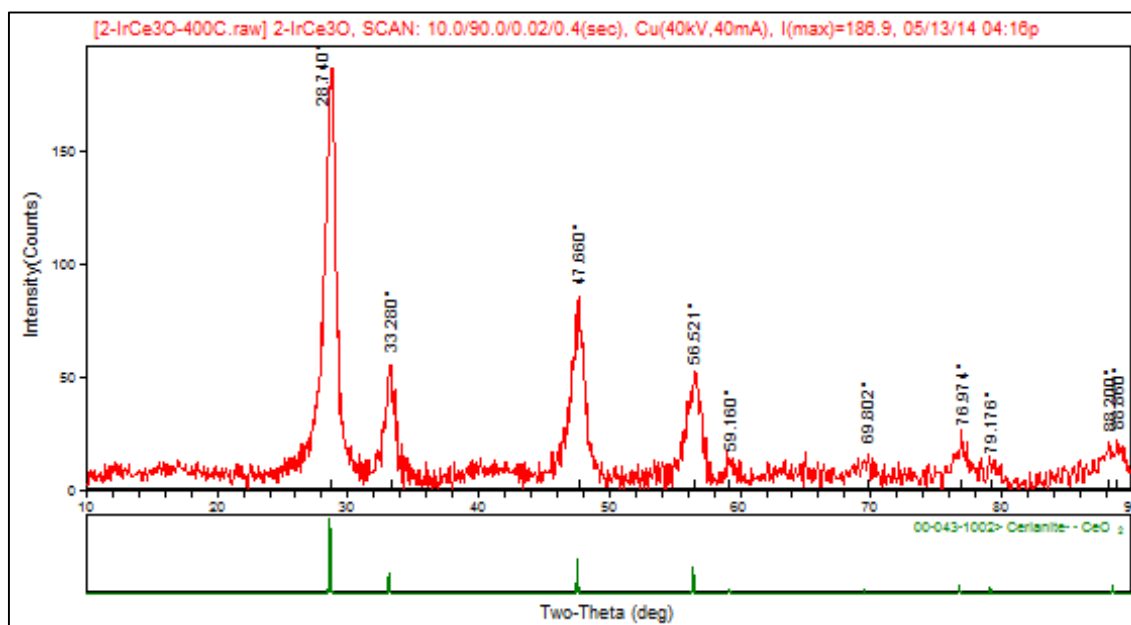


Figure 5.3 XRD pattern of 2-IrCe₃O_x synthesized at 400 °C and 6 hours

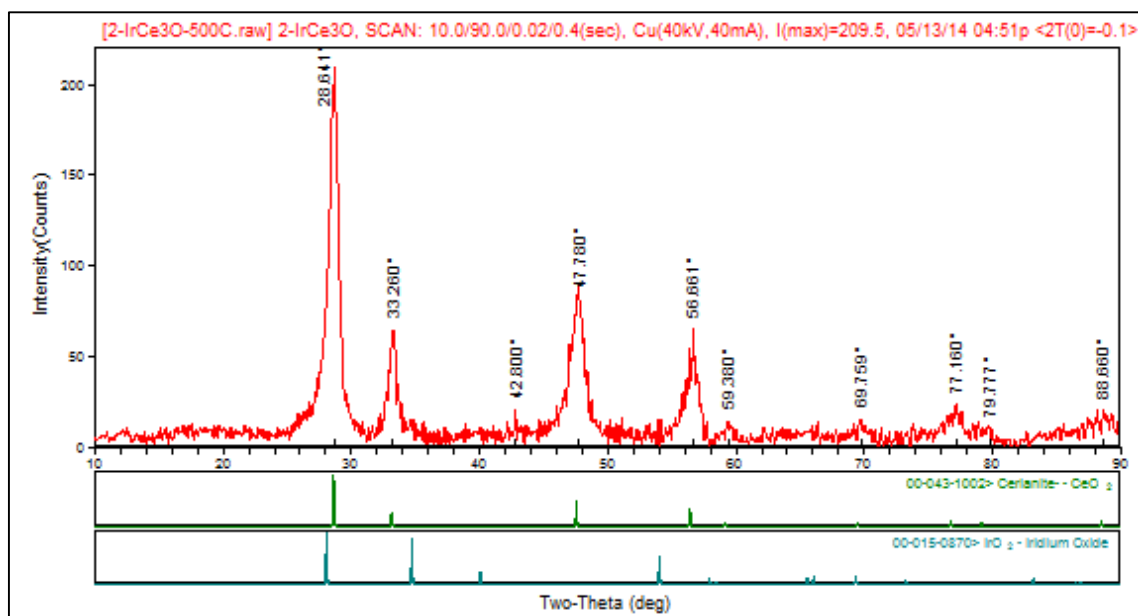


Figure 5.4 XRD pattern of 2-IrCe₃O_x synthesized at 500 °C and 6 hours

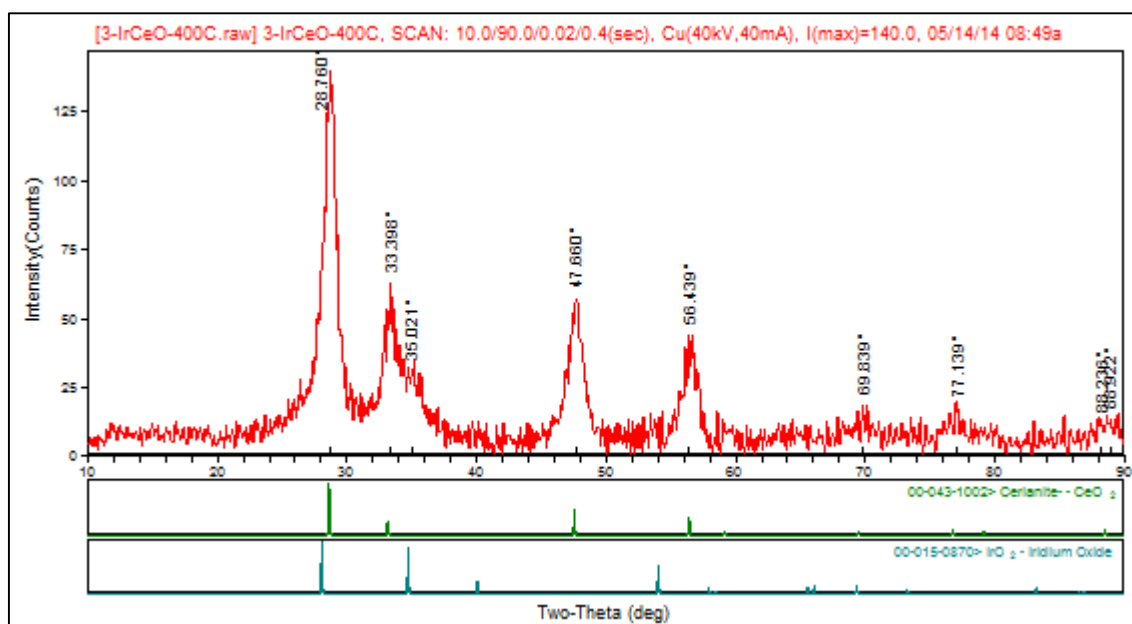


Figure 5.5 XRD pattern of 3-IrCeO_x synthesized at 400 °C and 6 hours

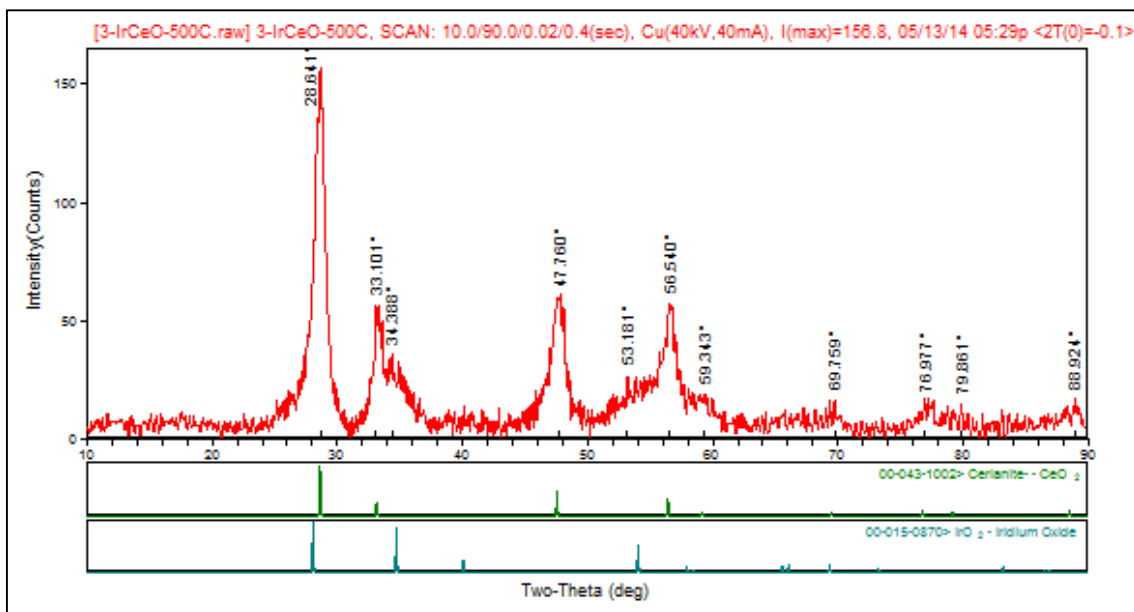


Figure 5.6 XRD pattern of 3-IrCe₃O_x synthesized at 500 °C and 6 hours

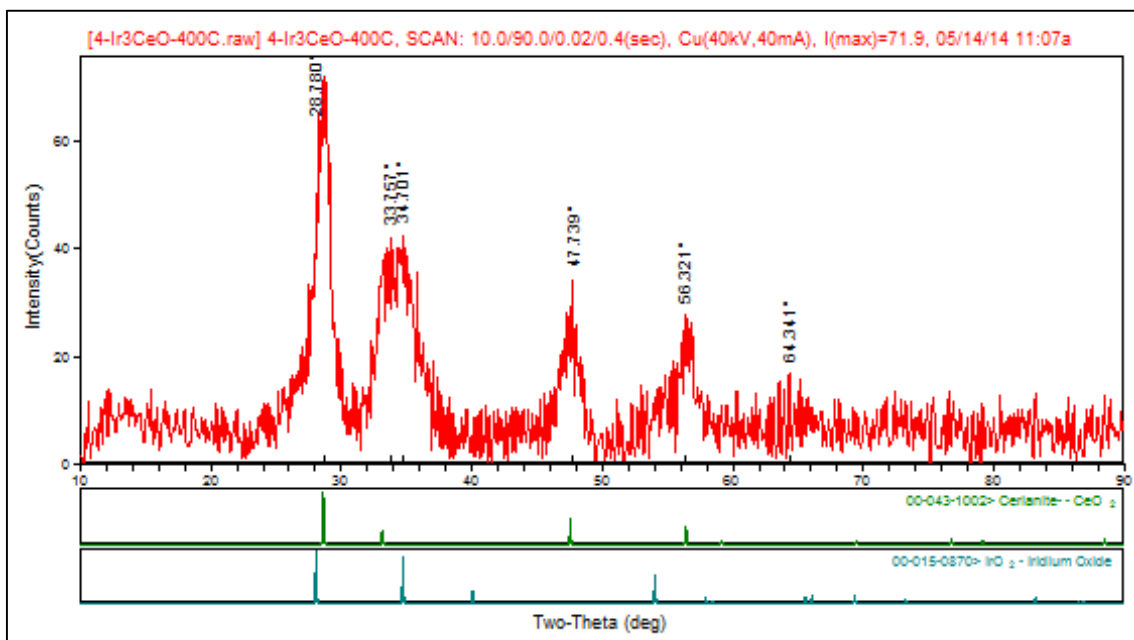


Figure 5.7 XRD pattern of 4-Ir₃CeO_x synthesized at 400 °C and 6 hours

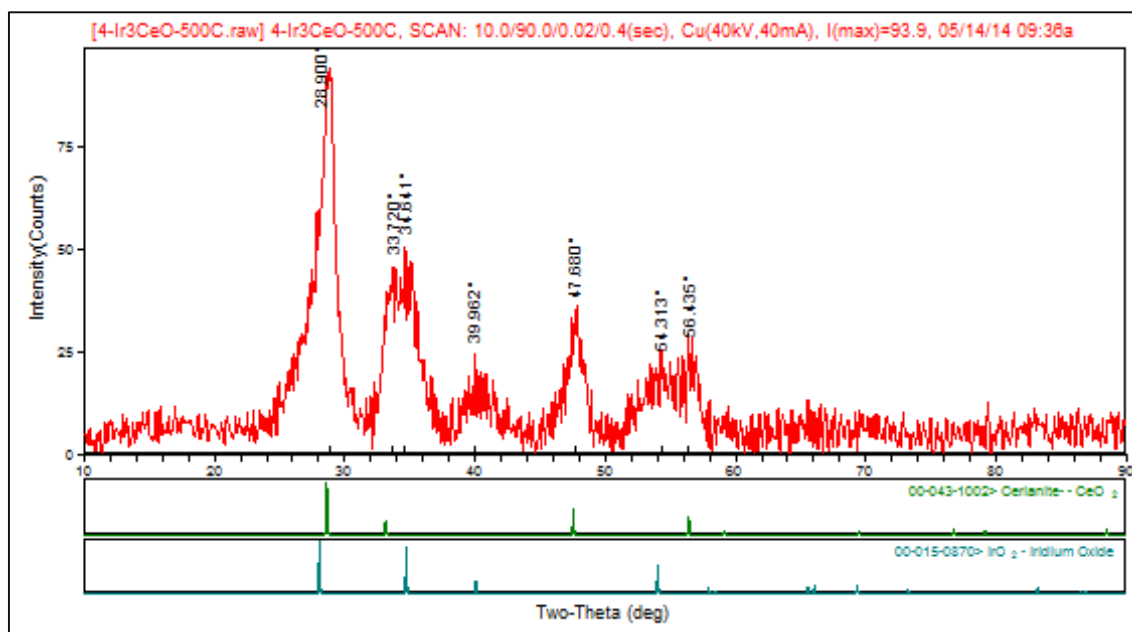


Figure 5.8 XRD pattern of 4-Ir₃CeO_x synthesized at 500 °C and 6 hours

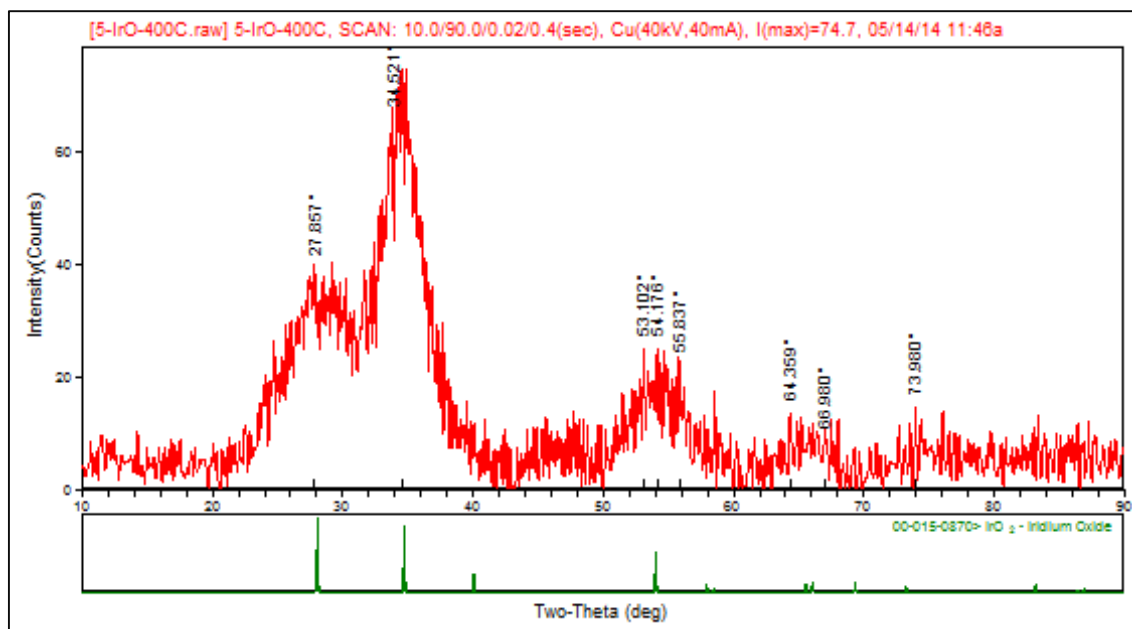


Figure 5.9 XRD pattern of 5-IrO_x synthesized at 400 °C and 6 hours

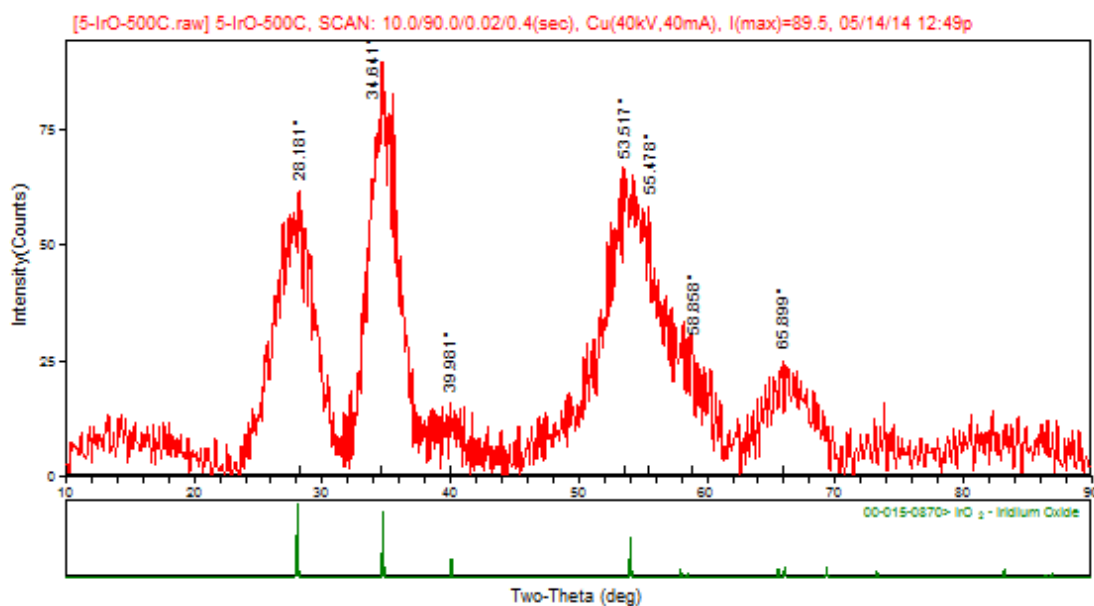


Figure 5.10 XRD pattern of 5-IrO_x synthesized at 500 °C and 6 hours

5.1.2. X-Ray Fluorescence (XRF) Analysis

Molar ratios of 2-IrCe₃O_x, 3-IrCeO_x and 4-Ir₃CeO_x can be identified by using XRF technique. After the XRF results it could be seen that the results match the molar ratios as it should be in reality. These findings could be seen at Table 5.3.

Table 5.3 XRF results of samples

Sample	Theoretical (%weight)		XRF Result (%weight)	
	Cerium	Iridium	Cerium	Iridium
IrCe₃O_x	70,15	29,87	69,29	30,71
IrCeO_x	43,92	56,07	43,34	56,66
Ir₃CeO_x	20,36	79,64	23,56	76,44

5.1.3. Brunauer Emmett Teller (BET) Surface Area Analysis

BET device has been used to determine the area of the synthesized catalyst support materials'. These surface area findings were compared with the commercial catalyst support material. Synthesized materials' surface area results are shown in Table 5.4.

Table 5.4 BET results of samples

		400 °C	500 °C	600 °C	650 °C
6 hours	1-CeO _x	36,36	10,96	6,95	
	2-IrCe ₃ O _x	84,30	36,66	34,54	
	3-IrCeO _x	86,86	74,46	64,74	
	4-Ir ₃ CeO _x	132,46	101,19	124,02	
	5-IrO _x	103,00	150,00	125,80	
8 hours	1-CeO _x	69,89	36,55	8,78	
	2-IrCe ₃ O _x	78,91	38,75	52,17	
	3-IrCeO _x	109,93	63,94	61,40	
	4-Ir ₃ CeO _x	109,93	123,32	92,66	
	5-IrO _x	102,70	139,90	100,6	
10 hours	1-CeO _x	23,11	16,64	---	---
	2-IrCe ₃ O _x	70,85	32,15	---	---
	3-IrCeO _x	87,86	74,58	---	---
	4-Ir ₃ CeO _x	86,61	130,16	---	---
	5-IrO _x	---	---	---	---

*Unit of results is m²/g

Vulcan XC-72: 207 m²/g

Measurements taken place at 600 °C has shown that samples exposed to 10 hours of heat treatment lose its surface area. That's the reason of there was no need to measure other samples which are treated under high temperature and long-time heat treatment. Measurements also have proven that short-term heat treated synthesized compounds tend to have higher surface area. In addition to that, the highest surface area has been achieved by only using the Ir₃CeO_x as the catalyst support material.

5.1.4. 4-Probe Conductivity Measurements

All catalyst support samples were pressed at 10 tones. After then, these samples were furnaced during 10 hours at under synthesis temperature. 4-Probe conductivity device has been used to determine the conductivity of the synthesized catalyst support

materials'. These conductivity findings were compared with the commercial catalyst support material. Synthesized materials' conductivity results are shown in Table 5.5.

Table 5.5 Four-Probe Conductivity Measurements results of samples

		400 °C	500 °C	600 °C	650 °C
6 hours	1-CeO _x	---	---	32,3*10 ⁻⁶	
	2-IrCe ₃ O _x	0,18	0,25	0,018	
	3-IrCeO _x	0,45	1,36	3,76	
	4-Ir ₃ CeO _x	2,54	2,17	1,26	
	5-IrO _x			3,10	
8 hours	1-CeO _x	---	3,98*10 ⁻⁶	---	
	2-IrCe ₃ O _x	0,58	0,60	0,78	
	3-IrCeO _x	5,60	1,38	1,26	
	4-Ir ₃ CeO _x	19,45	0,84	2,0*10 ⁻⁴	
	5-IrO _x	---	4,03	---	
10 hours	1-CeO _x	---	---	---	3,83*10 ⁻⁵
	2-IrCe ₃ O _x	0,033	0,15	0,11	4,8*10 ⁻³
	3-IrCeO _x	3,4*10 ⁻³	3,18	4,16	0,65
	4-Ir ₃ CeO _x	2,09	8,90	5,44	3,04
	5-IrO _x	8,74	---	---	8,10

*Unit of results is S/cm

Vulcan XC-72: 31 S/cm

This table illustrate that conductivity of sample increase with content of Iridium. Number 1 named samples have very low conductivity. It shows like insulator behavior. However, number 5 named samples have high conductivity. In light of these results, number 2, 3, 4 and 5 named samples show conductive behavior. Thus, they can use on PEM Fuel Cell as catalyst support.

XRD, XRF, BET and 4-Probe Conductivity measurement of result, we chosen IrCeO_x sample synthesised at 400 °C and 6 hours (3-400-6), IrCeO_x sample synthesised at 500 °C and 6 hours (3-500-6), Ir₃CeO_x sample synthesised at 400 °C and 6 hours (4-400-6), Ir₃CeO_x sample synthesised at 500 °C and 6 hours (4-500-6) to use durability measurement.

5.2. Synthesis of Pt/ CeO₂-IrO₂

Pt catalysts (45% weight) were synthesized on the prepared catalyst support materials. 50 ml of Dihydrogen Hexachloro Platinic acid (IV) ($\text{H}_2\text{PtCl}_6 \times 6 \text{H}_2\text{O}$) and 100 ml of water is stirred in magnetic stirrer. The diluted Ammonium Hydroxide (NH_3OH) is added, until the mixture's pH becomes 5. At the same time, support material and reducing agent solution (NaBH_4) are prepared. 10 ml of Ethanol-water solution is added to the 50 mg of support material. The solution is stirred in magnetic stirrer for 5 min. After then, it is mixed for 10 min in the ultrasonic bath and 1 min in the ultrasonic homogenizer. In another glass, 5 mg of NaBH_4 and 13 ml of water are stirred in magnetic stirrer and stored in the refrigerator, when lowered to right temperature. This NaBH_4 solution and the solution of support material are stirred in magnetic stirrer with ice water. This solution is mixed in the ultrasonic bath for 10 min. While mixing in the ultrasonic bath, heat increment is prevented.

Finally, the mixture is mixed in ultrasonic homogenizer with ice water. The support material and reducing agent are quickly mixed with platinumic acid, which has a pH of 5, in the magnetic stirrer. After 10 min of quickly stirring the mixture is placed in the ultrasonic bath. After this, the mixture is put aside for it to become stable. This process takes at least 3 hours. The mixture is vacuum filtered with Whatman 50 paper and washed 3 times with ethanol-water (2:3). The dried substance is ground with agate mortar and passed 60 mesh sieve. Vortex is used to speed up the sieve process. [20] All these processes can be seen at figure 5.11.

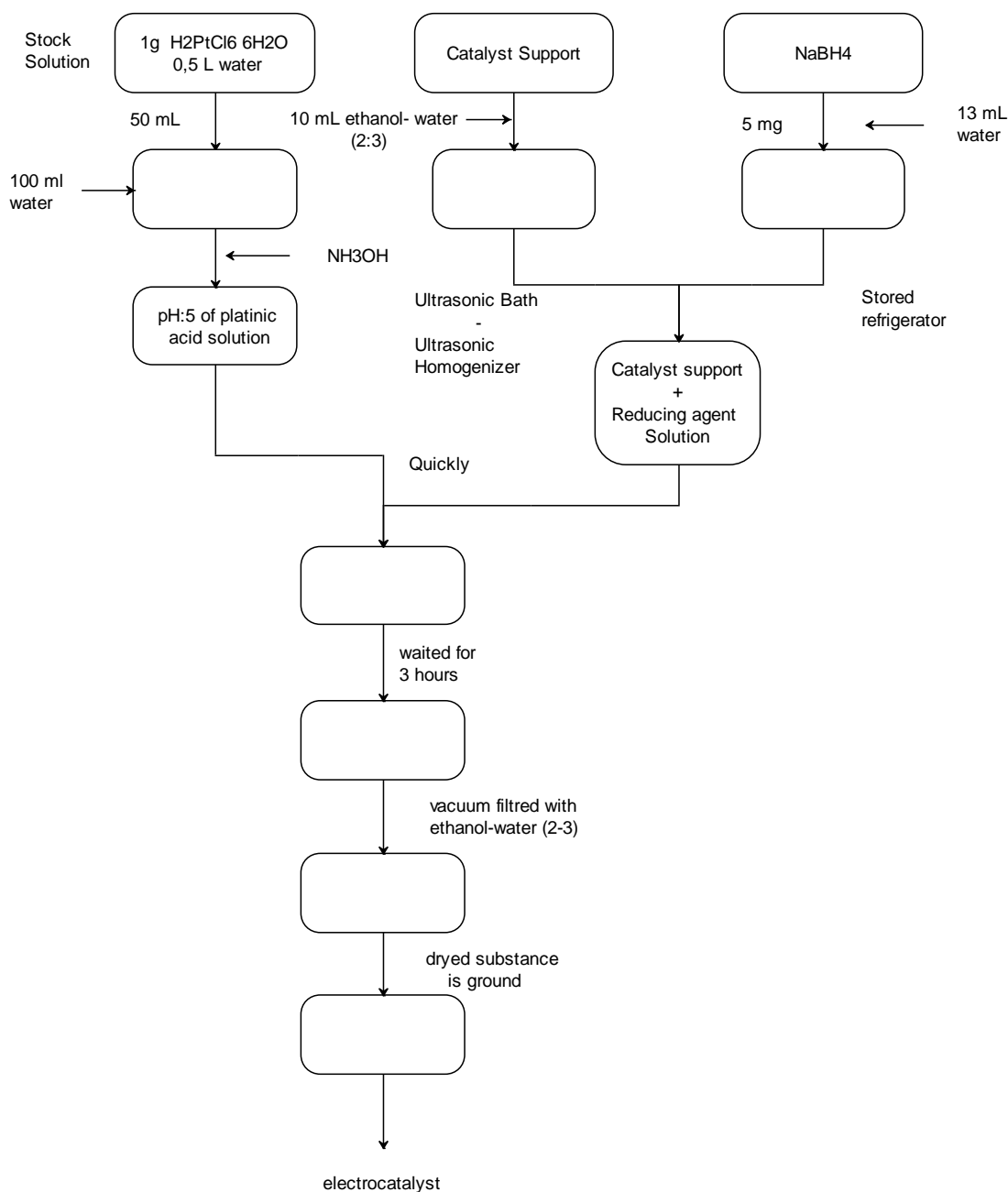


Figure 5.11 Process of Synthesis of Electrocatalyst

5.3. Synthesis of Pt-Au/ CeO₂-IrO₂

Pt-Au alloy catalysts were synthesized on the prepared support materials. Dihydrogen Hexachloro Platinic (IV) Hexahydrate ($\text{H}_2\text{PtCl}_6 \times 6 \text{H}_2\text{O}$ - 99,9%) and Gold (III) Chloride (AuCl_3) was used as Pt and Au precursors, respectively. Pluronic F-127 (Sigma Aldrich) was used as stabilizer to prevent agglomeration of catalyst particles. First of all, Pluronic F-127 was dissolved in deionized at 80 °C. Then aqueous solutions of H_2PtCl_6 and AuCl_3 was added to the stabilizer solution.

At the same time, the support material was dispersed in water with an ultrasonic bath. The catalyst precursor solution with the stabilizer was added on support material solution and the final mixture was mixed and homogenized with the ultrasonic bath. After that, the fresh made ascorbic acid was added to the mixture as a reducing agent. The final mixture was stirred in magnetic stirrer at high speed and homogenized in the ultrasonic bath for 1 hour. Then, it was vacuum filtered and washed with hot water to remove the stabilizer. The catalyst residue on the filter paper was removed from the filter paper and dried in vacuum oven at 100 °C, overnight. All these process can be seen at figure 5.12.

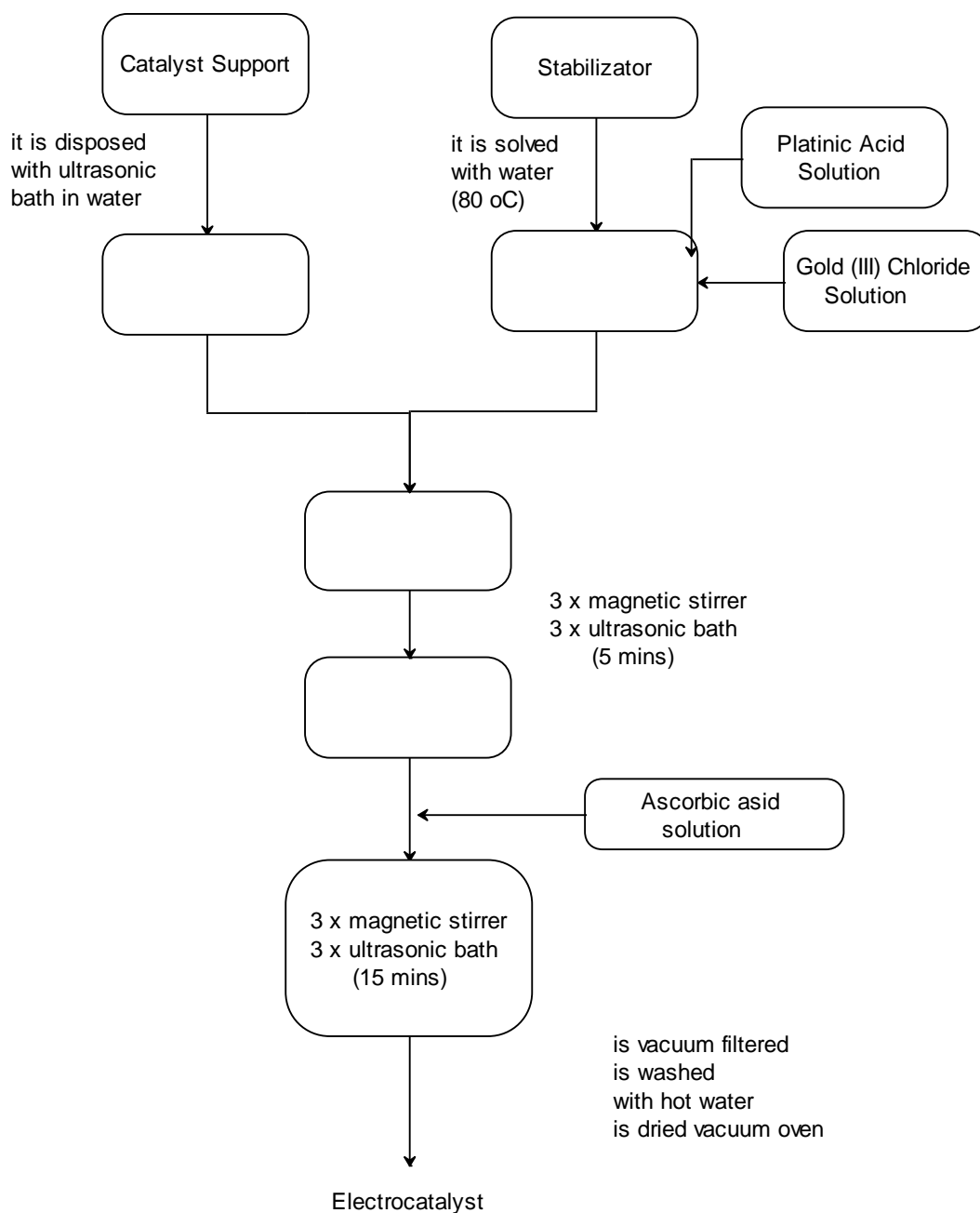


Figure 5.12 Process of Synthesis of Pt-Au Electrocatalyst

5.4. Oxygen Reduction Reaction Change of Kinetics Activity

Durability test was applied to create condition which cause performance drop, such as corrosion. During this test, potential was changed with 20 mV/s of scan rate in between 0,6 V and 1,2 V. Rotating voltammetry experiments were applied before and after from this accelerated test. Rotating voltammetry experiments carried out at 1600 rpm with 20 mV/s of scan rate in between -0,32- 1,0 V (vs. Ref). After this test, it was monitored that performance of catalyst layer dropped. These durability test findings were compared with the commercial catalyst support material. Synthesized materials' durability test results are shown in below.

Samples	Catalyst Support	Calcination Temperature	Calcination Time	% Pt (wt %)	% Au (wt %)
M34	3- CeIrO _x	400°C	6h	45	0
M35	3- CeIrO _x	500°C	6h	45	0
M44-1	4- CeIr ₃ O _x	400°C	6h	45	0
M45	4- CeIr ₃ O _x	500°C	6h	45	0
M44-2	4- CeIr ₃ O _x	400°C	6h	20	20

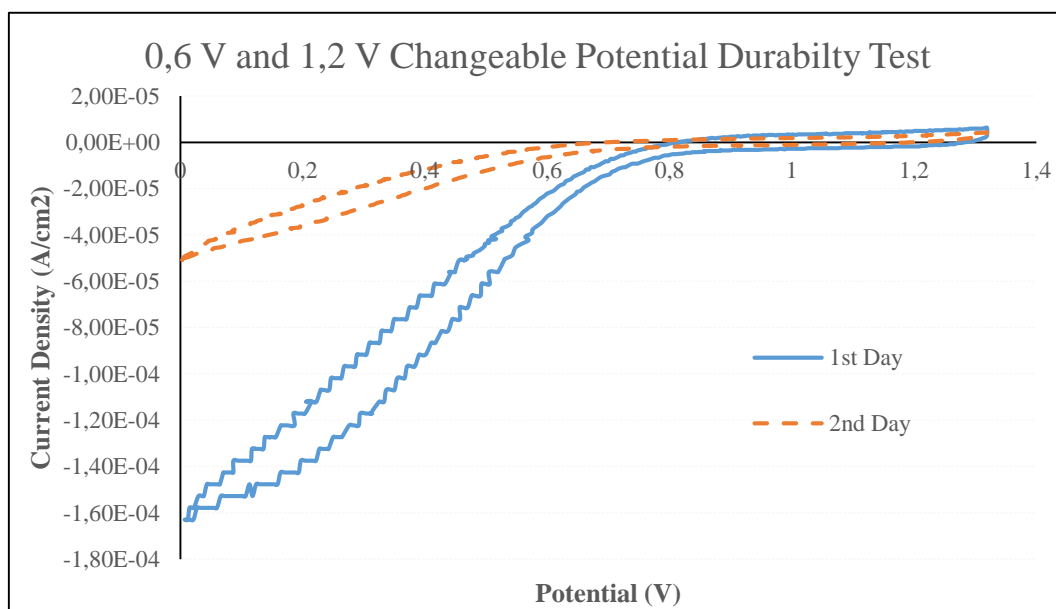


Figure 5.13 Rotating voltammetry experiment before and after the durability test for M34

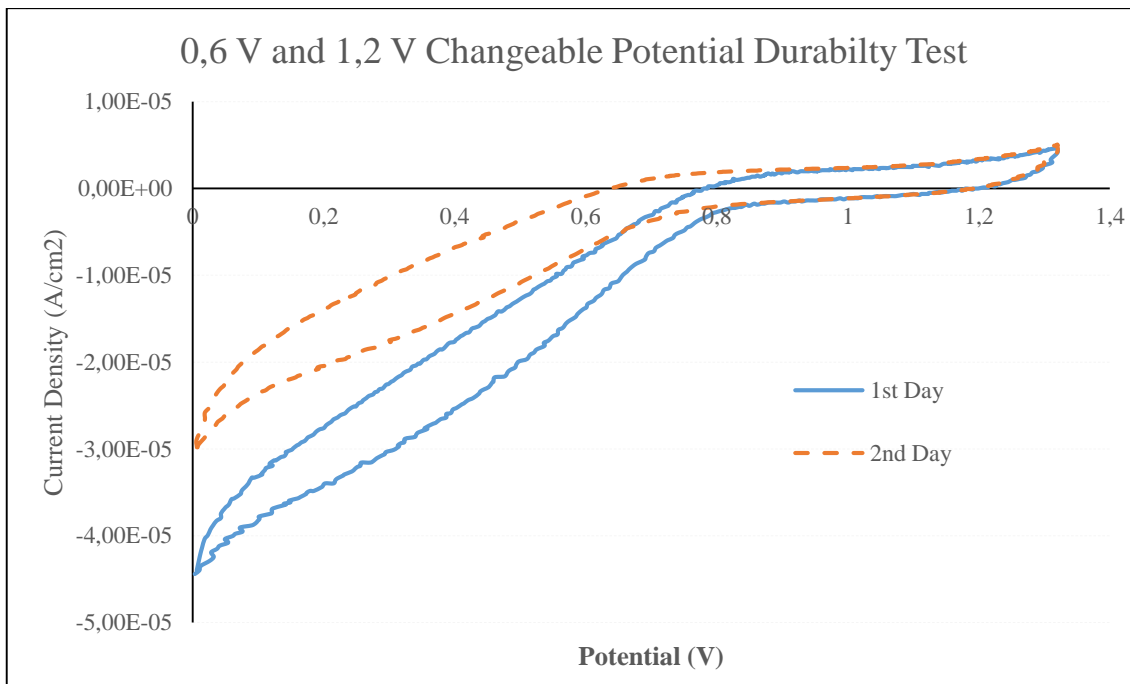


Figure 5.14 Rotating voltammetry experiment before and after the durability test for M35

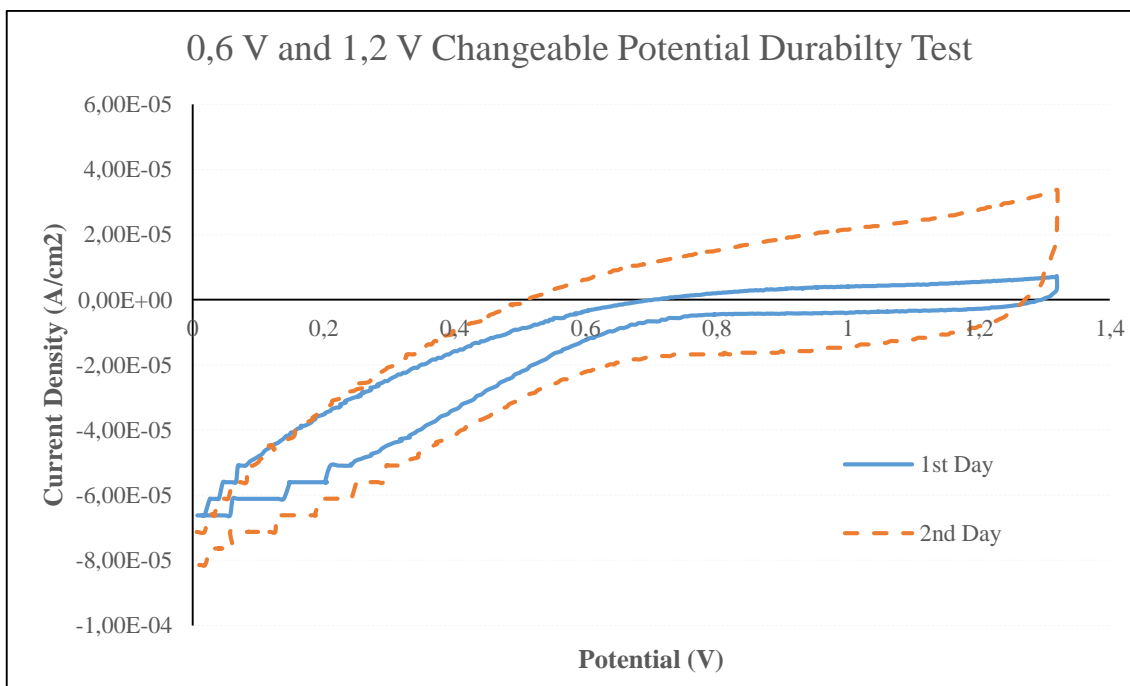


Figure 5.15 Rotating voltammetry experiment before and after the durability test for M44-1

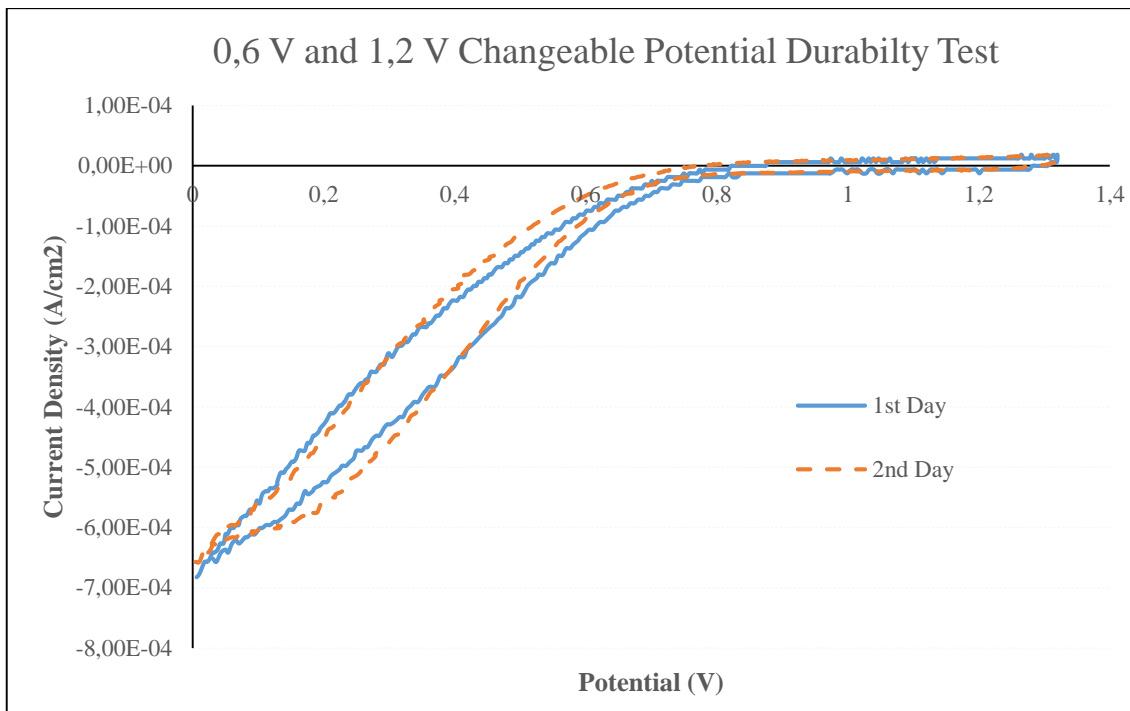


Figure 5.16 Rotating voltammetry experiment before and after the durability test for M45

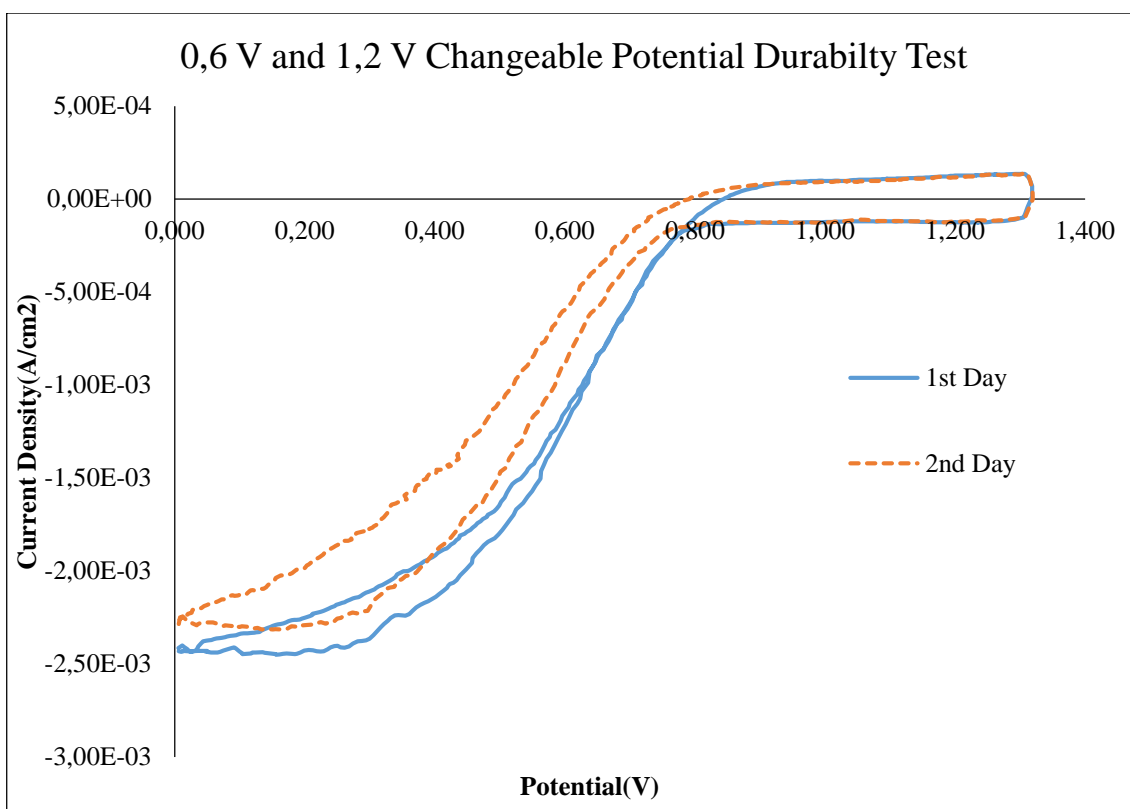


Figure 5.17 Rotating voltammetry experiment before and after the durability test for M44-2

Result of durability experiments, reduction of limit current after durability test can be calculated between 0,9 V and 0,85 V. The results can be compared with Vulcan XC-72. Synthesized materials' limit current, reduction of limit current and reduction of performance results are shown in below.

Table 5.6 Limit current density of samples

Catalyst Support	Limit Current Density (mA/cm²)	% Pt (wt %)	% Au (wt %)
Vulcan XC 72	3,50	45	0
M34 - 3-400-6	0,16	45	0
M35 - 3-500-6	0,04	45	0
M44 - 4-400-6	0,07	45	0
M45 - 4-500-6	0,68	45	0
M44-1 - 4-500-6	2,52	20	20

Result of limit current density, it can be seen that M44 and M45 named samples reach value which is competed with Vulcan XC-72.

Table 5.7 Reduction of limit current after durability test

Catalyst Support	Reduction of limit current density after durability test (%)	% Pt (wt %)	% Au (wt %)
Vulcan XC 72	8,4	45	0
M34	68,8	45	0
M35	34,9	45	0
M44-1	-14,3 (0)	45	0
M45	3,7	45	0
M44-2	7,5	20	20

Table 5.8 Reduction of kinetic current performance after durability test

Catalyst Support	Reduction of kinetic current performance after durability test (%)	% Pt (wt %)	% Au (wt %)
Vulcan XC 72	46,2	45	0
M34	78,2	45	0
M35	46,4	45	0
M44-1	-138,2 (0)	45	0
M45	4,9	45	0
M44-2	0,7	20	20

Exerted on catalysts after these tests, M45 and M44-2 named samples shown better durability than commercially Vulcan XC-72. In here, M44-1 named sample shown increasing of limit current and kinetic current performance. It may be evaluated that durability performance of this sample doesn't change during test.

CHAPTER 6

CONCLUSION

PEM type of fuel cells have a great potential to be a game-changer for an alternative energy production in various areas. However, cost and durability issues are obstacles for the commercialization of PEM Fuel Cells. Platinum catalyst not only affects the cost but also the performance.

Nowadays, as catalyst support material, we see that Vulcan XC-72 material is used in PEM type of fuel cells. Since this material is mostly based out of Carbon, in some extreme circumstances we see that performance drops dramatically. There is some other materials obviously needed to cover these inabilities, to change the odds. In this thesis study, some materials are synthesized as catalyst support material to determine a good replacement.

In this study, a novel mixed oxide catalyst support was investigated for use in PEM type of fuel cell, instead of Vulcan XC-72. A poisoning resisting CeO_2 matrix was doped with electrical conducting IrO_2 . Five different formulations of $\text{CeO}_2:\text{IrO}_2$ with molar ratios of 1:0, 0,75:0,25, 0,5:0,5, 0,25:0,75, and 0:1 were synthesized and tested. CeO_2 and IrO_2 in the 0,5:0,5, 0,25:0,75 of molar ratio were shown to have a high BET surface area $>80 \text{ m}^2/\text{g}$ as well as an excellent electrical conductivity of $\sim 1,5 \text{ S/cm}$. In light of these results, Cerium – Iridium Mixed Metal Oxides have enough property to use in PEM type of Fuel Cell.

Pt and Pt-Au deposition onto this Cerium-Iridium mixed oxides support was carried out via an impregnation – reduction method. The resultant electrocatalysts (20% Pt and 20% Pt-20% Au loading) was more stable than the commercial Pt/C baseline.

REFERENCES

- [1]. Barbir, F., *PEM Fuel Cells Theory and Practice*. Elsevier Academic Press, New York, 2005
- [2]. Cappadonia, M., et al., *Principles, Functions, and Classification of Fuel Cells*, in *Encyclopedia of Electrochemistry*. Wiley-VCH Verlag GmbH & Co. KGaA: New York, 2007
- [3]. Sandstede, G., et al., *History of low temperature fuel cells*, in *Handbook of Fuel Cells*. John Wiley & Sons, Ltd: New York, 2010
- [4]. Spiegel, C., *PEM Fuel Cell Modeling and Simulation Using Matlab*. Elsevier Academic Press, New York, 2008
- [5]. Ryan O'Hayre, S.-W.C., Whitney Colella, Fritz B. Prinz, *Fuel Cell Fundamentals*. 2nd ed. John Wiley & Sons, Ltd., New York, 2009
- [6]. Arnason, B. and T.I. Sigfusson, Iceland - a future hydrogen economy. *International Journal of Hydrogen Energy*. Vol. 25, pp. 389-394, 2000
- [7]. Hoogers, G., *Fuel cell technology handbook*. CRC press, 2002
- [8]. James Larminie, A.D., *Fuel Cell Systems Explained*. John Wiley & Sons, Ltd., 2003
- [9]. EG&G Technical Services, I., *Fuel Cell Handbook*. U.S. Department of Energy Office of Fossil Energy (DOE), National Energy Technology Laboratory, Washington D.C., 2004
- [10]. Lin, B.Y.S., D.W. Kirk, and S.J. Thorpe, Performance of alkaline fuel cells: A possible future energy system? *Journal of Power Sources*. Vol. 161, pp. 474-483, 2006
- [11]. Holland, B., J. Zhu, and L. Jamet. *Fuel cell technology and application*. in *Proceedings of Australasian Universities Power Engineering Conference (AUPEC'2001)*. 2001
- [12]. Zhang, J., *PEM Fuel Cell Electrocatalysts and Catalyst Layers*. 1 ed, ed. J. Zhang. Vol. 1. Springer Science and Business Media, Canada, 2008
- [13]. Panchenko, A., *Polymer Electrolyte Membrane Degradation and Oxidant Reduction in Fuel Cells: an EPR and DFT investigation*. Institute für Phyzikalische Chemie der Universitat, 2004

- [14]. Colón-Mercado, H.R. and B.N. Popov, Stability of platinum based alloy cathode catalysts in PEM fuel cells. *Journal of Power Sources*. Vol. 155, pp. 253-263, 2006
- [15]. Thanasilp, S. and M. Hunsom, Effect of Pt: Pd atomic ratio in Pt-Pd/C electrocatalyst-coated membrane on the electrocatalytic activity of ORR in PEM fuel cells. *Renewable Energy*. Vol. 36, pp. 1795-1801, 2011
- [16]. Ismail, M.S., et al., Effect of PTFE loading of gas diffusion layers on the performance of proton exchange membrane fuel cells running at high-efficiency operating conditions. *International Journal of Energy Research*. Vol. 37, pp. 1592-1599, 2013
- [17]. Hui, C., et al., Characteristics and Preparation of Polymer/Graphite Composite Bipolar Plate for PEM Fuel Cells. *Journal of composite materials*. Vol. 43, pp. 755-767, 2009
- [18]. Planes, E., L. Flandin, and N. Alberola, Polymer Composites Bipolar Plates for PEMFCs. *Energy Procedia*. Vol. 20, pp. 311-323, 2012
- [19]. Karimi, S., et al., A Review of Metallic Bipolar Plates for Proton Exchange Membrane Fuel Cells: Materials and Fabrication Methods. *Advances in Materials Science and Engineering*. Vol. 2012, pp. 1-22, 2012
- [20]. Dündar, F., *Synthesis of a Unique Catalysts as a Solution for the Agglomeration and Carbon Corrosion Problems and Improvement of the Fuel Cell Working Conditions in Material Science and Engineering*. Gebze Institute of Technology, 2011
- [21]. Büchi, F.N., M. Inaba, and T.J. Schmidt, *Polymer Electrolyte Fuel Cell Durability*. Springer Science + Business Media LLC, 2009
- [22]. Pourbaix, M., Applications of Electrochemistry in Corrosion Science and in Practice. *Corrosion Science*. Vol. 14, pp. 25-82, 1974
- [23]. Angerstein, H., B.E. Conway, and W.B.A. Sharp, Real Condition of Electrochemically Oxidized Platinum Surfaces .1. Resolution of Component Processes. *Journal of Electroanalytical Chemistry*. Vol. 43, pp. 9-36, 1973
- [24]. Conway, B.E., Electrochemical Oxide Film Formation at Noble-Metals as a Surface-Chemical Process. *Progress in Surface Science*. Vol. 49, pp. 331-452, 1995
- [25]. You, H., et al., Resonance X-ray scattering from Pt(111) surfaces under water. *Physica B-Condensed Matter*. Vol. 283, pp. 212-216, 2000
- [26]. Sasaki, K., M. Shao, and R. Adzic, *Dissolution and Stabilization of Platinum in Oxygen Cathodes*, in *Polymer Electrolyte Fuel Cell Durability*, F.N. Büchi, M. Inaba, and T.J. Schmidt, Editors. Springer Science + Business Media LLC. pp. 7-27, 2009
- [27]. Schmidt, T.J., Characterization of High-Surface-Area Electrocatalysts Using a Rotating Disk Electrode Configuration. *Journal of The Electrochemical Society*. Vol. 145, pp. 2354, 1998

- [28]. Kinoshita, K. and J.A.S. Bett, Potentiodynamic analysis of surface oxides on carbon blacks. *Carbon*. Vol. 11, pp. 403-411, 1973
- [29]. Kumar, A. and V.K. Ramani, RuO₂-SiO₂ mixed oxides as corrosion-resistant catalyst supports for polymer electrolyte fuel cells. *Applied Catalysis B: Environmental*. Vol. 138-139, pp. 43-50, 2013
- [30]. Saha, M.S., et al., High electrocatalytic activity of platinum nanoparticles on SnO₂ nanowire-based electrodes. *Electrochemical and Solid-State Letters*. Vol. 10, pp. B130-B133, 2007
- [31]. Huang, S.-Y., et al., Development of a Titanium Dioxide-Supported Platinum Catalyst with Ultrahigh Stability for Polymer Electrolyte Membrane Fuel Cell Applications. *Journal of the American Chemical Society*. Vol. 131, pp. 13898-13899, 2009
- [32]. Ioroi, T., et al., Corrosion-Resistant PEMFC Cathode Catalysts Based on a Magnéli-Phase Titanium Oxide Support Synthesized by Pulsed UV Laser Irradiation. *Journal of The Electrochemical Society*. Vol. 158, pp. C329, 2011
- [33]. Chhina, H., S. Campbell, and O. Kesler, An oxidation-resistant indium tin oxide catalyst support for proton exchange membrane fuel cells. *Journal of Power Sources*. Vol. 161, pp. 893-900, 2006
- [34]. Chen, K.Y., Effect of Nafion Dispersion on the Stability of Pt/WO₃ Electrodes. *Journal of The Electrochemical Society*. Vol. 143, pp. 2703, 1996
- [35]. Raghuvver, V. and B. Viswanathan, Synthesis, characterization and electrochemical studies of Ti-incorporated tungsten trioxides as platinum support for methanol oxidation. *Journal of Power Sources*. Vol. 144, pp. 1-10, 2005
- [36]. Maiyalagan, T. and B. Viswanathan, Catalytic activity of platinum/tungsten oxide nanorod electrodes towards electro-oxidation of methanol. *Journal of Power Sources*. Vol. 175, pp. 789-793, 2008
- [37]. Zhang, Y., et al., Investigation of self-humidifying membranes based on sulfonated poly(ether ether ketone) hybrid with sulfated zirconia supported Pt catalyst for fuel cell applications. *Journal of Power Sources*. Vol. 168, pp. 323-329, 2007
- [38]. Ioroi, T., et al., Sub-stoichiometric titanium oxide-supported platinum electrocatalyst for polymer electrolyte fuel cells. *Electrochemistry Communications*. Vol. 7, pp. 183-188, 2005
- [39]. Haas, O.E., et al., Synthesis and characterisation of Ru_xTi_{1-x}O₂ as a catalyst support for polymer electrolyte fuel cell. *Journal of New Materials for Electrochemical Systems*. Vol. 11, pp. 9-14, 2008
- [40]. Lo, C.-P., et al., TiO₂-RuO₂ electrocatalyst supports exhibit exceptional electrochemical stability. *Applied Catalysis B: Environmental*. Vol. 140-141, pp. 133-140, 2013
- [41]. Subban, C.V., et al., Sol-Gel Synthesis, Electrochemical Characterization, and Stability Testing of Ti_{0.7}W_{0.3}O₂ Nanoparticles for Catalyst Support Applications in Proton-Exchange Membrane Fuel Cells. *Journal of the American Chemical Society*. Vol. 132, pp. 17531-17536, 2010

- [42]. Lo, C.P. and V. Ramani, SiO(2)-RuO(2): a stable electrocatalyst support. *ACS Appl Mater Interfaces*. Vol. 4, pp. 6109-16, 2012
- [43]. Borup, R., et al., Scientific Aspects of Polymer Electrolyte Fuel Cell Durability and Degradation. *Chemical Reviews*. Vol. 107, pp. 3904-3951, 2007
- [44]. Liu, H., et al., *Chemical Degradation: Correlations Between Electrolyzer and Fuel Cell Findings*, in *Polymer Electrolyte Fuel Cell Durability*, F.N. Büchi, M. Inaba, and T.J. Schmidt, Editors. Springer Science + Business Media: Newton. pp. 71-118, 2009
- [45]. Hermann, A., T. Chaudhuri, and P. Spagnol, Bipolar plates for PEM fuel cells: A review. *International Journal of Hydrogen Energy*. Vol. 30, pp. 1297-1302, 2005
- [46]. Scherer, J., D. Münter, and R. Ströbel, *Influence of Metallic Bipolar Plates on the Durability of Polymer Electrolyte Fuel Cells*, in *Polymer Electrolyte Fuel Cell Durability*, F.N. Büchi, M. Inaba, and T.J. Schmidt, Editors. Springer Science + Business Media LLC. pp. 243-255, 2009
- [47]. Jacob Spendelow, J.M., *2013 Annual Progress Report*, in *Fuel Cell Cost-2013*. U.S. Department of Energy, 2013
- [48]. Adams, R. and R.L. Shriner, Platinum Oxide as a Catalyst in the Reduction of Organic Compounds. Iii. Preparation and Properties of the Oxide of Platinum Obtained by the Fusion of Chloroplatinic Acid with Sodium Nitrate¹. *Journal of the American Chemical Society*. Vol. 45, pp. 2171-2179, 1923